Experimental Air-broadened Line Parameters in the ν_2 Band of CH_3D

Adriana Predoi-Cross, Shannon Brawley-Tremblay, Chad Povey

Physics Department, University of Lethbridge

4401 University Drive, Lethbridge, AB, T1K 3M4 Canada

and Mary Ann H. Smith

Science Directorate, NASA Langley Research Center, MS 401A, Hampton, VA 23681-2199, USA

Send correspondence to:

Dr. A. Predoi-Cross

Department of Physics, University of Lethbridge, 4401 University Drive,

Lethbridge, AB, T1K 3M4 Canada

Phone: 403-329-2697 Fax: 403-329-2057 E-mail address: Adriana.predoicross@uleth.ca

PACS classification: 33.20.Ea, 39.30+w

ABSTRACT

In this study we report the first experimental measurements of air-broadening and air-induced pressure-shift coefficients for approximately 378 transitions in the ν_2 fundamental band of CH_3D. These results were obtained from analysis of 17 room temperature laboratory absorption spectra recorded at 0.0056 cm^{-1} resolution using the McMath-Pierce Fourier transform spectrometer located on Kitt Peak, Arizona. Three absorption cells with path lengths of 10.2, 25 and 150 cm were used to record the spectra. The total sample pressures ranged from 0.129×10^{-2} to 52.855×10^{-2} atm with CH_3D volume mixing ratios of approximately 0.0109 in air. The spectra were analyzed using a multispectrum non-linear least-squares fitting technique. We report measurements for air pressure-broadening coefficients for transitions with quantum numbers as high as $J'' = 20$ and $K = 15$, where $K'' = K' \equiv K$ (for a parallel band). The measured air-broadening coefficients range from 0.0205 to 0.0835 cm^{-1} atm^{-1} at 296 K. All the measured pressure-shift coefficients are negative and are found to vary from about –0.0005 to –0.0080 cm^{-1} atm^{-1} at the temperature of the spectra. We have examined the dependence of the measured broadening and shift parameters on the J'', and K quantum numbers and also developed empirical expressions to describe the broadening coefficients in terms of m ($m = -J''$, J'' and $J'' + 1$ in the ^{Q}P-, ^{Q}Q-, and ^{Q}R-branch, respectively) and K. On average, the empirical expressions reproduce the measured broadening coefficients to within 4.4%.

INTRODUCTION

Laboratory spectroscopic studies of the vibrational bands of CH_3D are needed for the correct interpretation of terrestrial and planetary atmospheric spectra. Accurate measurements of the positions, intensities, pressure-broadening and pressure-induced shift coefficients of CH_3D spectral transitions are essential for quantitative analysis involving the abundance and the D/H ratio in methane (via the CH_3D/CH_4 ratio) in the atmospheres of these Solar System bodies [1-7].

This paper is a continuation of our study of spectroscopic line parameters in the ν_2 band of CH_3D [8-10]. The ν_2 band of $^{12}CH_3D$ is the lowest band ($\nu_0 \approx 2200$ cm^{-1}) of a polyad of nine interacting vibrational states. Several studies of line shape parameters for CH_3D perturbed by air have been reported. Recently, studies of air-broadening and shifting in the ν_3, ν_5, and ν_6 bands of CH_3D have been published [11-13]. Devi et al. [14] measured N_2- and air-broadening coefficients for 24 lines and self-broadening coefficients for 2 lines in the ν_6 band at room temperature. N_2-, air-, and self- broadening coefficients for several transitions in the ν_3 band were measured by Devi et al. [15]. Walrand et al. [16] reported N_2- and O_2-broadening coefficients also measured by fitting the spectral profiles of transitions in the ν_3 band to both Voigt and Rautian models. The O_2-broadening coefficients for 29 transitions in the in the ^{Q}P and ^{Q}R branches of the ν_3 band were retrieved [17] by fitting Voigt and Rautian profiles to the spectral lines recorded with a diode laser spectrometer. The results were then compared with collisional broadening results calculated using semiclassical impact theory. Lacome et al. [18] have published the N_2-, H_2-, and self-broadening parameters for 10 transitions in the ν_6 band. The N_2-, self-, H_2-, and He-broadening coefficients for 4 transitions in the ν_6 band at temperatures of 123, 188, and 295 K were reported by Varanasi and Chudamani [19]. An

empirical expression for N_2-broadening coefficients in the ν_2 band of CH3D has been reported by Varanasi et al. [20]. Chudamani and Varanasi [21] measured the N_2-broadening coefficients of 5 ^{Q}P-branch transitions in the ν_2 band of CH_3D over the 94–300 K.

In the present study, we report extensive, high-quality measurements of air broadening and pressure-induced shift coefficients for 378 transitions between 2048 and 2318 cm^{-1} in the ν_2 band of CH_3D. We have analyzed spectra recorded with the high-resolution Fourier transform spectrometer located at the National Solar Observatory on Kitt Peak, Arizona. We have compared our measurement results with calculated air-broadening and air-pressure shift coefficients based on our CH_3D-N_2 and CH_3D-O_2 calculations [9,10]. The theoretical broadening and pressure shift coefficients were computed using our calculated parameters for CH_3D-N_2 and CH_3D-O_2 mixtures reported in Refs. 9 and 10. The theoretical broadening and shift parameters in CH_3D-N_2 [9] and CH_3D-O_2 [10] mixtures are calculated using the semiclassical formulation of Robert and Bonamy [22].

EXPERIMENTAL DETAILS

The seventeen pure gas and air-broadened absorption spectra used in this work were recorded at an unapodized resolution of 0.0056 cm^{-1} using the McMath-Pierce Fourier transform spectrometer (FTS) of the National Solar Observatory (NSO) on Kitt Peak, Arizona. The experimental conditions for the self-broadened spectra have been reported in Ref. 8. In Table 1 we present only the experimental conditions for the air-broadened spectra used in this study. Three absorption cells with path lengths of 10.2, 25 and 150 cm were used in the experiments. The spectra covering the 2048–2318 cm^{-1} were simultaneously fit using a multispectrum non-linear least-squares procedure [23]. Using this analysis tool we were able to combine spectra

recorded with low pressures of 98% pure CH_3D, self-broadened spectra and lean mixtures (~1%) of CH_3D in air in a single non-linear least-squares solution. This methodology avoids having to give highly accurate input values for line intensities, self-broadening and self-induced pressure shifts. Instead, these parameters are determined from the pure gas spectra during the multispectrum fit. The experimental setup and data reduction methods were described in detail in our study to self-broadening and self-induced pressure shifts of CH_3D [8]. Residual water vapor lines appeared in all of our spectra as a combination of low pressure absorption due to small amounts of residual water vapor present in the vacuum tank enclosing the FTS, and H_2O absorption arising from water vapor in the N_2-purged atmospheric paths between the source and the absorption cell and between the absorption cell and the entrance aperture of the interferometer. The wavenumber calibration for the CH_3D line positions was performed with respect to the line centers [24] of residual water lines. Examples of spectral ^{Q}P-branch, ^{Q}Q-branch and ^{Q}R-branch intervals for transitions with J'' = 8 and K values from 0 to 7 are presented in Fig. 1.

RESULTS AND DISCUSSION

The CH_3D absorption spectra were analyzed using a multispectrum analysis software developed by D.C. Benner and documented in Ref. 23. As previously reported [25] the retrievals of broadening coefficients from the absorption spectra are complicated by possible instrumental distortions and by the need to properly reproduce the wings of the spectral lines. The multispectrum fit software models the spectral lines using the Voigt line shape function convolved with the instrument line shape function appropriate for the McMath-Pierce FTS used to record the spectra. The software makes corrects for truncation and field of view effects. The

realistic FTS instrumental line shape function is a sinc function convolved with the aperture function. It was calculated based on the iris diameter, focal length of the collimating lens for the McMath-Pierce FTS instrument, maximum optical path difference and the field of view of the instrument. The sampling grid used to model the spectra was chosen to be very close to the halfwidth of the narrowest feature in our spectra. Oversampling of the modeled spectra can be accompanied by an artificial enlargement of the spectral domain on which computations are made [26. The software used in this analysis uses calculated Doppler widths of the spectral lines [25]. The line parameters for each measured line were determined by fitting intervals of 2 - 10 cm^{-1} wide in all spectra simultaneously. The differences between the experimental spectra and the calculated spectra were minimized by adjusting various line parameters through non-linear least-squares fitting.

The air-broadening coefficients and air-pressure induced shift coefficients for CH_3D transitions in the ν_2 band retrieved from our multispectrum analysis are presented in Table 2. The errors quoted in parentheses represent two standard deviation uncertainties in the measured quantities in units of the last quoted digit. These errors represent twice the uncertainties as obtained from the multispectrum least-squares fits. By reporting twice the standard deviation uncertainties we hope to take into account any systematic errors arising from other sources such as calibration standards, pressure and temperature determinations and mixing ratio uncertainties are difficult to asses.

The air-broadening coefficients are given in units of cm^{-1} atm^{-1} at 296 K. For each transition we list the line center positions retrieved from the fits (in cm^{-1}) and the transitions quantum numbers. In our analysis we have not applied any temperature corrections to the measured pressure-shift coefficients. Hence, the pressure-shift coefficients listed in Table 2

correspond to values at the mean temperature (298 ± 2 K) at which the spectra were recorded. A small temperature correction was applied to the air-broadening coefficients using the temperature dependence coefficients reported in the HITRAN database. We present our results arranged in groups of ^{Q}P-, ^{Q}Q-, and ^{Q}R-branches. Within each branch, the results are arranged separately for the A- and E-species transitions.

Discussion of the measured air-broadening coefficients

The values of the observed air-broadening coefficients listed in Table 2 range from 0.0205 to 0.0835 $cm^{-1}atm^{-1}$ at 296 K. The air-broadening coefficients as a function of m ($m = -J''$, J'', $J'' + 1$ for ^{Q}P-, ^{Q}Q-, and ^{Q}R-branch lines, respectively) and are presented in Fig. 2. The air-broadening coefficients for the majority of ν_2 transitions decrease slowly with increasing m. The unusual pattern of the air-broadening coefficients for ^{Q}Q-branch transitions with $J'' = K$ has been pointed out with a different symbol.

In Fig. 3 we have plotted the ratio of our measured air-broadening coefficients to the air-broadening coefficients with the same quantum numbers belonging to another parallel vibrational band in CH_3D, namely the ν_3 band [11]. The mean ratio of air-broadening coefficients is 1.01(3), consistent with the belief that broadening coefficients are independent of vibrational band.

Our measured air-broadening coefficients may be used to develop highly-accurate theoretical modeling of broadening coefficients. Until such theoretical results are available, we propose the use of three empirical expressions to estimate the air broadening coefficients of transitions in the ν_2 band that have not been measured yet.

Following the approach from Refs. 8-10 we have fitted the experimental air-broadening coefficients to empirical expressions. The broadening coefficients for all transitions except $J'' = K$ and $J'' = K+1$ in the ^{Q}Q-branch, were fitted to the following expression:

$$\gamma(\text{air}) = c_0 + c_1|m|(|m| + 1) + c_2K^2. \quad (1)$$

For the fit with 303 lines, the average percentage difference between the experimental and calculated broadening coefficients (using Eq. 1 and the parameters in Table 3) is 4.6 %. The magnitude of c_2 is about 1.75 times that of c_1 which suggests that the air-broadening coefficients have a stronger dependence on K rather then on m.

In the ^{Q}Q branch for the $J'' = K$ transitions the broadening coefficients were expressed as

$$\gamma = c_0 + c_1|m|(|m| + 1) + c_2|m|^2(|m| + 1)^2 \quad (2)$$

As again determined by a least-squares fit to the data, the constants c_0, c_1, and c_2 are also given in Table 3. The percentage difference between the experimental and calculated broadening coefficients (using Eq. 2 and parameters in Table 3) for the fit with 11 transitions is 1.2%.

We noticed that the ^{Q}Q branch transitions with the $J'' = K+1$ also follow a distinctive pattern and have fitted them to Eq. 2. The c_0, c_1, and c_2 constants for this last fit are also given in Table 3. The percentage difference between the experimental and calculated broadening coefficients (using Eq. 2 and parameters in Table 3) for the fit with 12 transitions with the $J'' = K+1$ is 2.8%. Overall, on average the empirical expressions reproduce the measured broadening coefficients to 4.4%. The extrapolation and use of this empirical model to determine the broadening coefficients far outside the quantum number range of these measurements may not offer reliable values.

Discussion of the measured air-induced pressure-shift coefficients

The results of this study listed in Table 2 show that within our measurement uncertainties all measured pressure shift coefficients are negative. The measured pressure-shift coefficients vary between –0.0005 and –0.0080 cm^{-1} atm^{-1} at the temperature of the spectra. In Figure 4 we have plotted the measured air-induced pressure-shift coefficients as a function of *m*. 4. The trend with *m* of air-induced pressure-shift coefficients for ^{Q}Q-branch $J'' = K$ transitions is not as clearly defined as for the corresponding air-broadening coefficients presented in Fig. 2. Overall, the pressure shifts for ^{Q}Q-branch transitions with $J'' = K$ are smaller than shifts with the same *m* value but different *K* values.

Comparison of measured air-broadening coefficients with theoretical data

In this work we have compared our measured air-broadening coefficients with theoretical calculations for air-broadening coefficients. We calculated the theoretical air-broadening coefficients using the expression:

$$\gamma(\text{air}) = 0.79 \times \gamma(N_2) + 0.21 \times \gamma(O_2) \quad (3)$$

where the theoretical N_2- and O_2-broadening coefficients are taken from Refs. 9 and 10. These coefficients have been calculated using the semi-classical model of Robert and Bonamy [22] under the assumption that CH_3D behaves like a linear molecule for its interaction with N_2 or O_2.

The measured and theoretical results γ(air) as a function of $|m|$ for selected *K* transitions in the ^{Q}P-, ^{Q}Q-, and ^{Q}R-branches are presented in Fig.5. Also included is a typical error bar. The theoretical results of the broadening coefficients are also in overall good agreement with the experimental data for transitions with $|m| \geq 12$. For transitions with $|m| = K+1$ approaching the theoretical broadening coefficients are generally significantly underestimated .

The measured and theoretical air-broadening coefficients, γ(air), as a function of K for constant $|m|$ are plotted in Fig. 6. The typical error bar displayed in Figure 6 is the same as in Figure 5. The overall agreement between the measured and calculated broadening coefficients is good. However, as K approaches $|m|$, the agreement worsens and the theoretical results are probably underestimated.

Comparison of measured air-pressure shift coefficients with theoretical data

The air-pressure shift coefficients δ(air) have been calculated at 296 K for lines in the ^{Q}P-, ^{Q}Q-, and ^{Q}R- branches of the ν_2 band using the theoretical results reported in Refs. 9 and 10 and the following expression:

$$\delta(\text{air}) = 0.79 \times \delta(N_2) + 0.21 \times \delta(O_2) \quad (4)$$

The air-pressure shift coefficients are plotted in Fig. 7 as a function of $|m|$. The ^{Q}R-branch coefficients for low K show an interesting trend where they change from small negative values at low $|m|$ towards more negative values with a minimum in the vicinity of $|m|$ = 7 to 11. At higher $|m|$ values the shift coefficients begin to increase towards less negative values, resulting in a concave up shape to the graphs. The ^{Q}R-branch lineshift coefficients for K = 0 and 1 are less positive than for higher K values and are nearly constant over the range of $|m|$ values. The ^{Q}P-branch shift coefficients follow a different trend with $|m|$. It is difficult to recognize a trend in the ^{Q}Q-branch transitions due to the relatively small number of data points.

The air-shift coefficients also show interesting trends with K, as presented in Fig. 8. The theoretical calculations reproduce the tendency of the ^{Q}R-branch shift coefficients to increase with decreasing K fairly well. The ^{Q}R-branch shift coefficients display again a concave up shape with minimum around K = 2. The general trend in the measured and theoretical ^{Q}P-branch shift

coefficients is to remain nearly constant for low K values, then to fall off rapidly to more negative values as K approaches $|m|$.

CONCLUSION

This study represents a significant step toward a better understanding of air-broadening in CH_3D. This is the first experimental study that reports air-broadening and air-shifting in the ν_2 vibrational band of CH_3D. We report accurate values for zero pressure line center positions, air-broadening coefficients and air pressure - induced shift coefficients for 378 transitions. Several interesting patterns in the measured pressure-broadening and pressure-induced shift coefficients have been observed and discussed. Overall, the empirical expressions derived to compute the air-broadening coefficients as a function of $|m|$ and K reproduce our measurements within 4.4%, will be useful for remote sensing applications.

ACKNOWLEDGMENTS

We are very grateful to Dr. Linda R. Brown from the Jet Propulsion laboratory (JPL), California Institute of Technology for allowing us to use her self-broadened CH_3D spectra. Our gratitude also goes to Dr. D. Chris Benner from the College of William and Mary for offering his multispectrum fit program. We thank Dr. Malathy Devi from the College of William and Mary for her advice in handling the spectra and the analysis with the multispectrum fit program. A. Predoi-Cross acknowledges the support she received from the National Sciences and Engineering Research Council of Canada and the University of Lethbridge Research Fund. We also thank NASA's Upper Atmosphere Research Program for their support of the McMath-Pierce FTS laboratory facility.

REFERENCES

1. V. Kunde, R. Hanel, W. Maguire, D. Gautier, J.P. Baluteau, A. Marten, A. Chedin, N. Husson and N. Scott, Astrophys. J. **263**, 443 (1982).

2. A. Coustenis, B. Bezard, D. Gautier, Icarus **82**,67 (1989).

3. G. Orton G, J. Lacy, J. Achtermann and P. Parmar, Bull. Amer. Astron. Soc. **22**, 1093 (1990).

4. F.W. Irion, E.J. Moyer, M.R. Gunson, C.P. Rinsland, Y.L.Yung, H.A. Michelsen, R.J. Salawitch, A.Y. Chang, M.J. Newchurch, M.M. Abbas, M.C. Abrams and R. Zander, Geo. Res. Lett. **23**, 2381 (1996).

5. M.D. Smith, B.J. Conrath and D. Gautier, Icarus **124**, 598 (1996).

6. T. Fouchet and E. Lellouch, Icarus **144**, 114 (2000).

7. O. Mousis, D. Gautier and A. Coustenis, Icarus **159**, 156 (2002).

8. A. Predoi-Cross, K. Hambrook, M. Brawley-Tremblay, J.-P. Bouanich, M.V. Devi, D.C. Benner and L.R. Brown, J. Mol. Spectrosc. **234,** 53 (2005).

9. A. Predoi-Cross, K. Hambrook, M. Brawley-Tremblay, J.-P. Bouanich and M.A.H. Smith, J. Mol. Spectrosc. **234**, 312 (2005).

10. A. Predoi-Cross, K. Hambrook, S. Brawley-Tremblay, J.-P. Bouanich, M.V. Devi and M.A.H. Smith, J. Mol. Spectrosc. **236**, 75 (2006).

11. M.V. Devi, D.C. Benner, M.A.H. Smith, C.P. Rinsland and L.R. Brown, J. Quant. Spectrosc. Radiat. Transfer **517**–**518**, 455 (2000).

12. M.V. Devi, D.C. Benner, M.A.H. Smith and C.P. Rinsland, J. Quant. Spectrosc. Radiat. Transfer **68**, 135 (2001).

13. M.V. Devi, D.C. Benner, M.A.H. Smith and C.P. Rinsland, J. Quant. Spectrosc. Radiat. Transfer **68**, 1 (2001).

14. M.V. Devi, D.C. Benner, M.A.H. Smith, C.P. Rinsland and K.B. Thakur, J. Mol. Spectrosc. **122**, 182 (1987).

15. M.V. Devi, C.P. Rinsland , D.C. Benner, M.A.H. Smith and K.B. Thakur, Appl. Opt. **25**, 1848 (1986).

16. J. Walrand, G. Blanquet and J.-P. Bouanich, Spectrochim. Acta A **52**, 1037 (1996).

17. K. Jacquiez, G. Blanquet, J. Walrand and J.-P. Bouanich, J. Mol. Spectrosc. **171**, 525 (1995).

18. N. Lacome, F. Cappellani, G. Restelli, Appl. Opt. **26**, 766 (1987).

19. P. Varansai, S. Chudamani, Appl. Opt. **28** 2119 (1989).

20. P. Varanasi, L.P. Giver, F.P.J. Valero, J. Quant. Spectrosc. Radiat. Transfer **30** 511 (1983).

21. S. Chudamani, P. Varanasi, J. Quant. Spectrosc. Radiat. Transfer **38** 179 (1987).

22. D. Robert and J. Bonamy, J. Phys. (Paris) **40**, 923 (1979).

23. D.C. Benner, C.P. Rinsland, V.M. Devi, M.A.H. Smith and D. Atkins, J. Quant. Spectrosc. Radiat. Transfer **53**, 705 (1995).

24. R.A. Toth, J. Opt. Soc. Am. B. **8,** 2236 (1991).

25. M.A.H. Smith, C.P. Rinsland, B. Fridovich and K. Narahari Rao, Molecular Spectroscopy: Modern Research, III, Academic Press, Orlando, chap. 3 (1985).

26. S.A. Teukolsky, W.T. Vetterling, B.P. Flannery, Numerical Recipes in Fortran 90, The Art of Parallel Scientific Computing, Volume 2, William H. Press (1996).

TABLE CAPTIONS

Table 1. Summary of Experimental Conditions of CH_3D spectra

Table 2. Measured and calculated zero-pressure line positions, air-broadening coefficients and air-induced pressure-shift coefficients in the ν_2 band of CH_3D.

Table 3. Coefficients for the empirical expansions of the broadening parameters (Eqs. 1 and 2) in the ν_2 band.

FIGURE CAPTIONS

1. ^{Q}P-branch, ^{Q}Q-branch and ^{Q}R-branch spectral intervals for transitions with J'' = 8 and K values up to 7. The spectrum was recorded using the 150 cm long gas cell and a gas pressure of 1.342×10^{-3} atm.

2. Measured air-broadening coefficients, γ(air), (cm^{-1} atm^{-1} at 296 K) in the ^{Q}P-, ^{Q}Q- and ^{Q}R-branches as a function of m. The $J'' = K$ transitions in the ^{Q}Q-branch are plotted with diamond symbols highlighting the rapidly falling trend of the corresponding air-broadening coefficients with m.

3. Comparisons between the air-broadening coefficients obtained in the present study and those obtained by Devi et al. [11].

4. Measured air-induced pressure-shift coefficients, δ(air), (cm^{-1} atm^{-1} at the temperature of the spectra) as a function of m.

5. Variation of air-broadening coefficients with $|m|$ for (A) K = 3; (B) K = 6; (C) K = 0; (D) K = 1; (E) K = 2 and (F) K = 4. For a given $|m|$, the theoretical broadening coefficients for the ^{Q}P and ^{Q}R lines are very nearly the same.

6 Variation of air-broadening coefficients, γ(air), versus K in select $|m|$ series ($|m|$ = 7 to 12) in the ^{Q}P-, ^{Q}Q-, and ^{Q}R-branches.

7. Measured and theoretical air-induced pressure-shift coefficients, δ(air), as a function of $|m|$ for transitions with selected K values: (A) K = 3, (B) K = 6, (C) K = 1, (D) K = 2, (E) K = 4 and (F) K = 5.

8. Measured and theoretical air-induced pressure-shift coefficients, δ(air) as a function of K for (A) $|m|$ = 7, (B) $|m|$ = 8, (C) $|m|$ = 9, (D) $|m|$ = 10, (E) $|m|$ = 11, and (F) $|m|$ = 12.

Figure 1

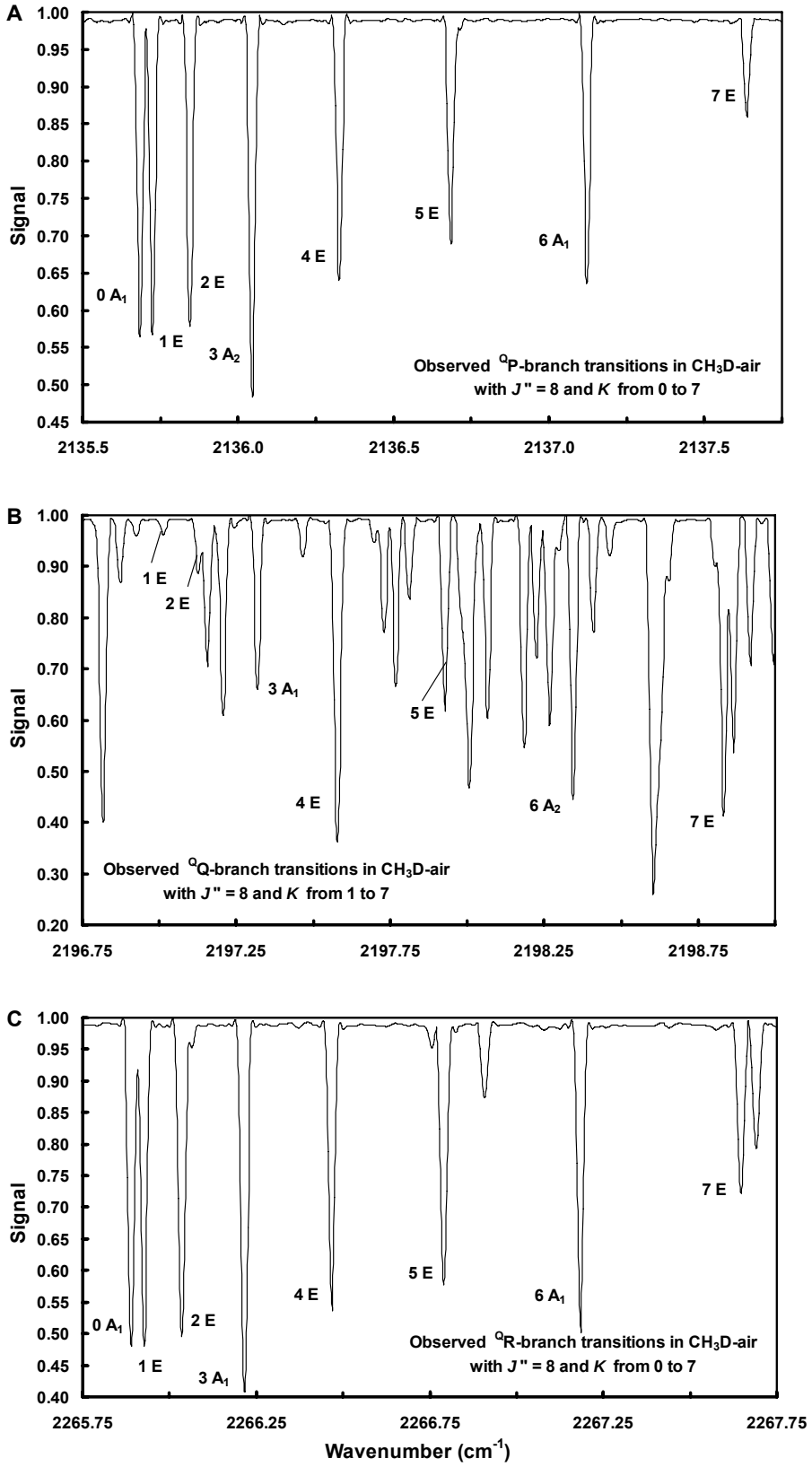
A
B
C
Signal
Wavenumber (cm-1)
0 A1
1 E
2 E
3 A2
4 E
5 E
6 A1
7 E
Observed QP-branch transitions in CH3D-air
with J" = 8 and K from 0 to 7
3 A1
6 A2
Observed QQ-branch transitions in CH3D-air
with J" = 8 and K from 1 to 7
Observed QR-branch transitions in CH3D-air
with J" = 8 and K from 0 to 7

Figure 2

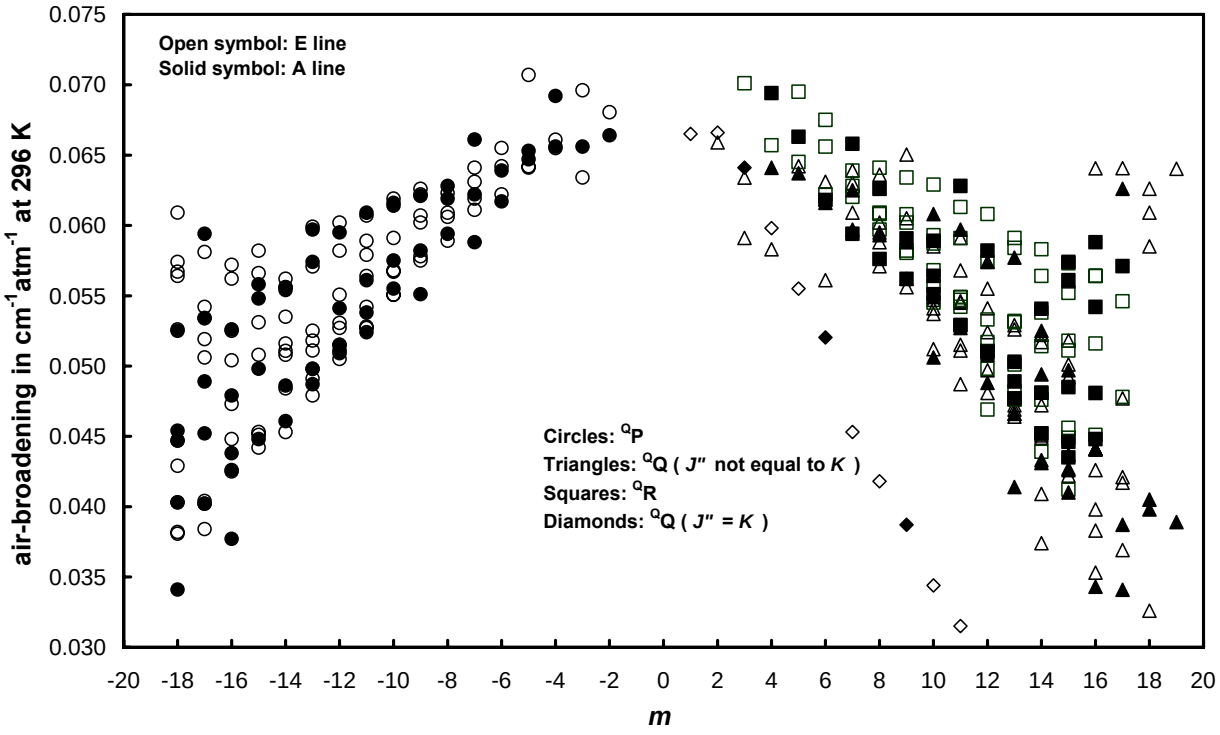
Open symbol: E line
Solid symbol: A line
Circles: ^QP
Triangles: ^QQ (J″ not equal to K)
Squares: ^QR
Diamonds: ^QQ (J″ = K)
air-broadening in cm^-1atm^-1 at 296 K
m
0.075
0.070
0.065
0.060
0.055
0.050
0.045
0.040
0.035
0.030
-20 -18 -16 -14 -12 -10 -8 -6 -4 -2 0 2 4 6 8 10 12 14 16 18 20

Figure 3

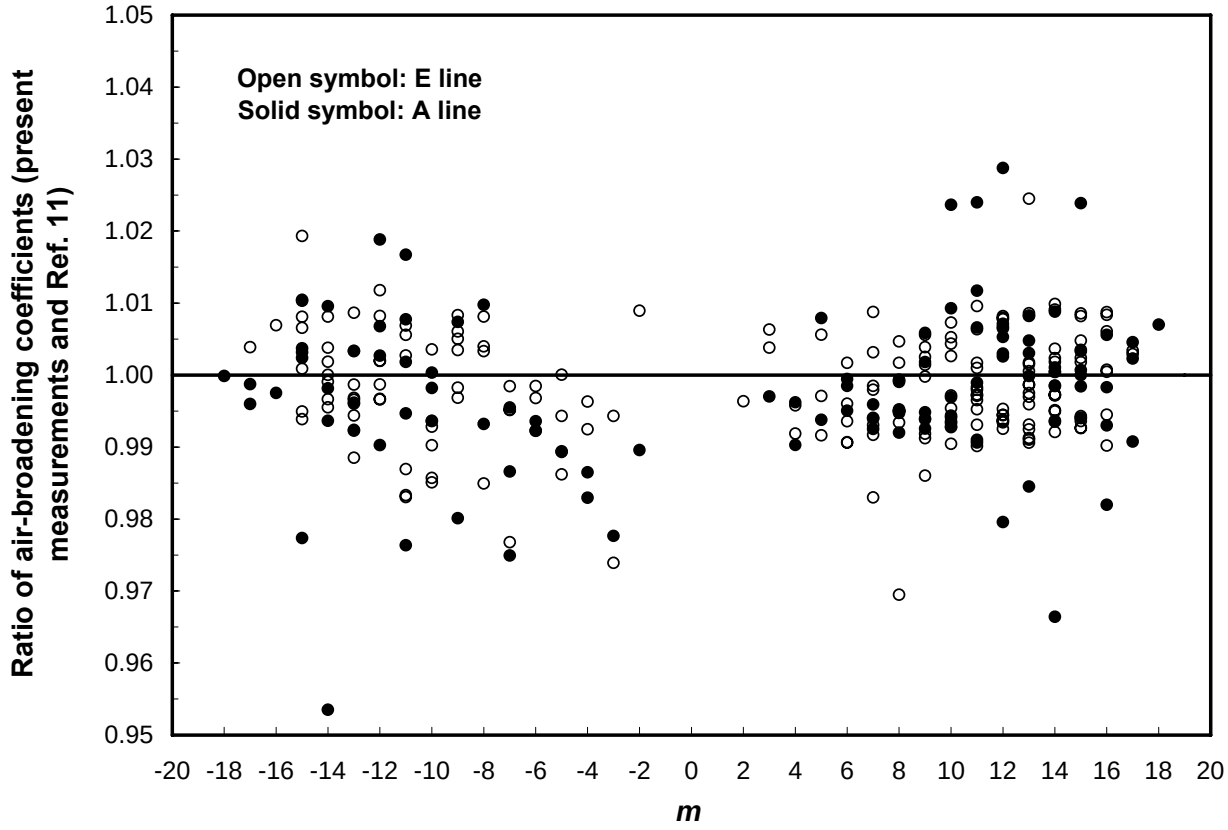
Open symbol: E line
Solid symbol: A line
Ratio of air-broadening coefficients (present measurements and Ref. 11)
m
1.05
1.04
1.03
1.02
1.01
1.00
0.99
0.98
0.97
0.96
0.95
-20 -18 -16 -14 -12 -10 -8 -6 -4 -2 0 2 4 6 8 10 12 14 16 18 20

Figure 4

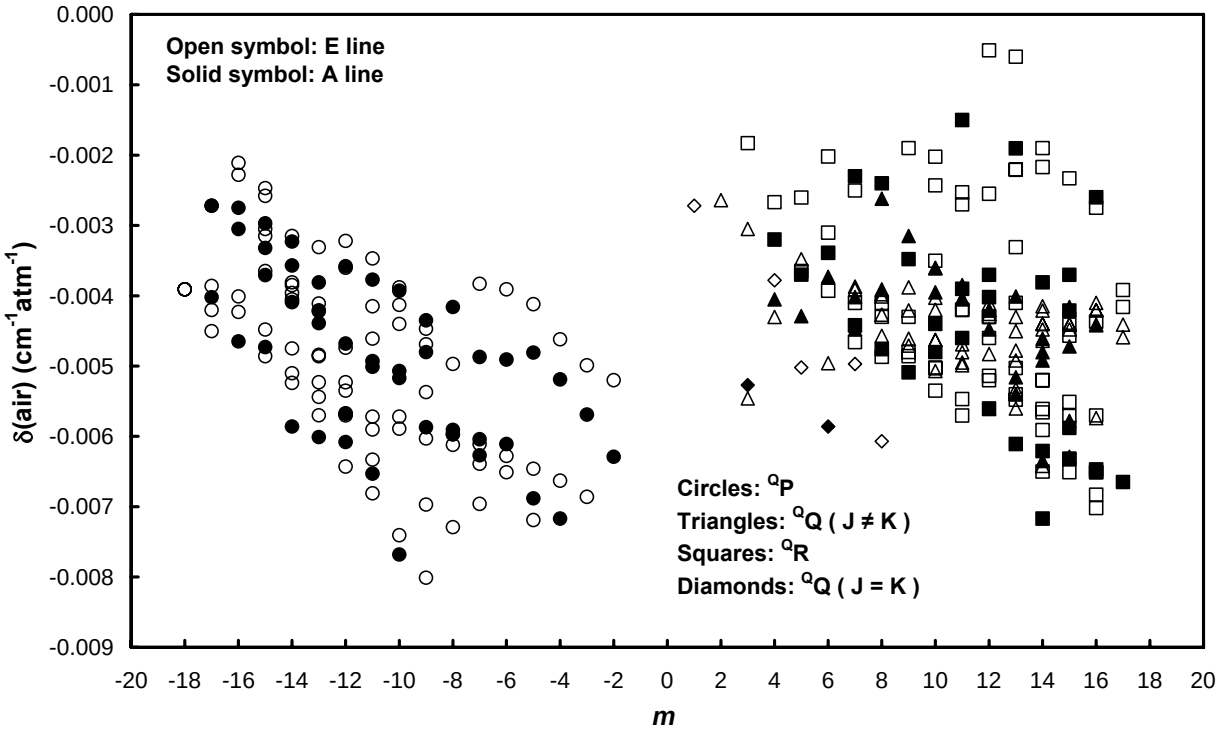
Open symbol: E line
Solid symbol: A line
Circles: ^{Q}P
Triangles: ^{Q}Q (J ≠ K)
Squares: ^{Q}R
Diamonds: ^{Q}Q (J = K)
δ(air) (cm^{-1}atm^{-1})
m
0.000
-0.001
-0.002
-0.003
-0.004
-0.005
-0.006
-0.007
-0.008
-0.009
-20 -18 -16 -14 -12 -10 -8 -6 -4 -2 0 2 4 6 8 10 12 14 16 18 20

Figure 5

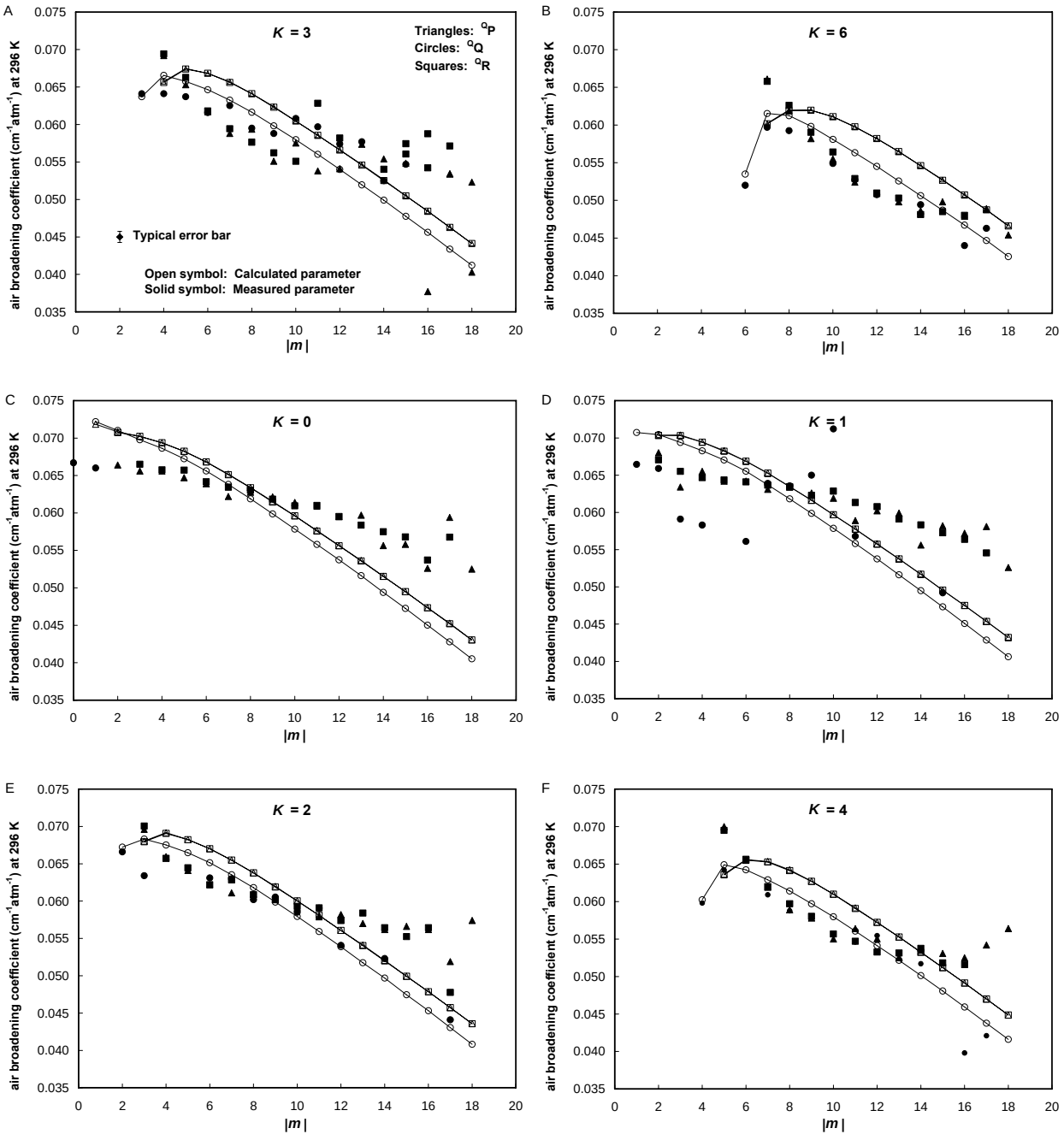
A
K = 3
Triangles: ᵒP
Circles: ᵒQ
Squares: ᵒR
Typical error bar
Open symbol: Calculated parameter
Solid symbol: Measured parameter
B
K = 6
C
K = 0
D
K = 1
E
K = 2
F
K = 4
air broadening coefficient (cm⁻¹atm⁻¹) at 296 K
|m|

Figure 6

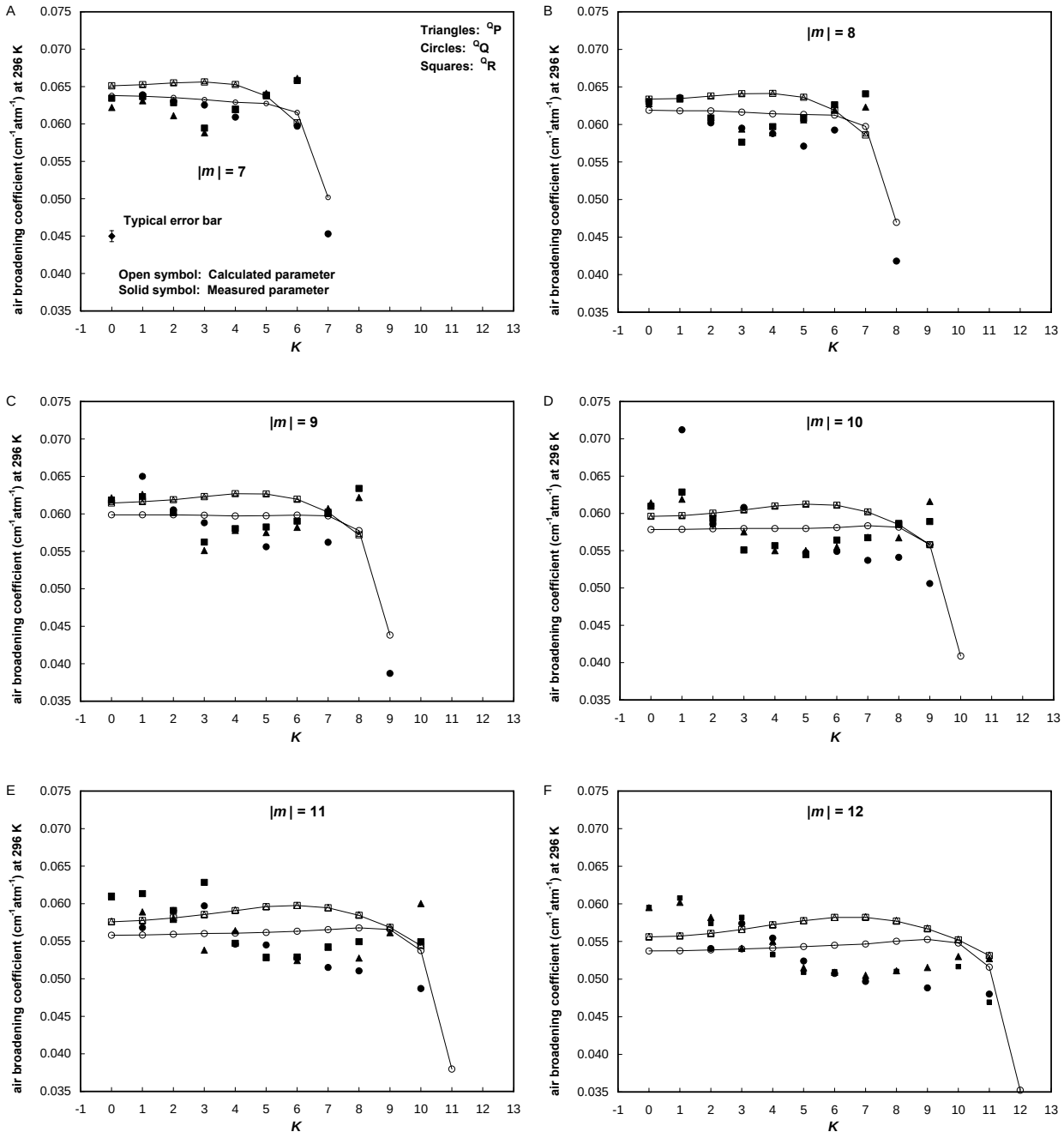
A
B
C
D
E
F
air broadening coefficient (cm-1atm-1) at 296 K
K
Triangles: OP
Circles: OQ
Squares: OR
|m| = 7
|m| = 8
|m| = 9
|m| = 10
|m| = 11
|m| = 12
Typical error bar
Open symbol: Calculated parameter
Solid symbol: Measured parameter

Figure 7

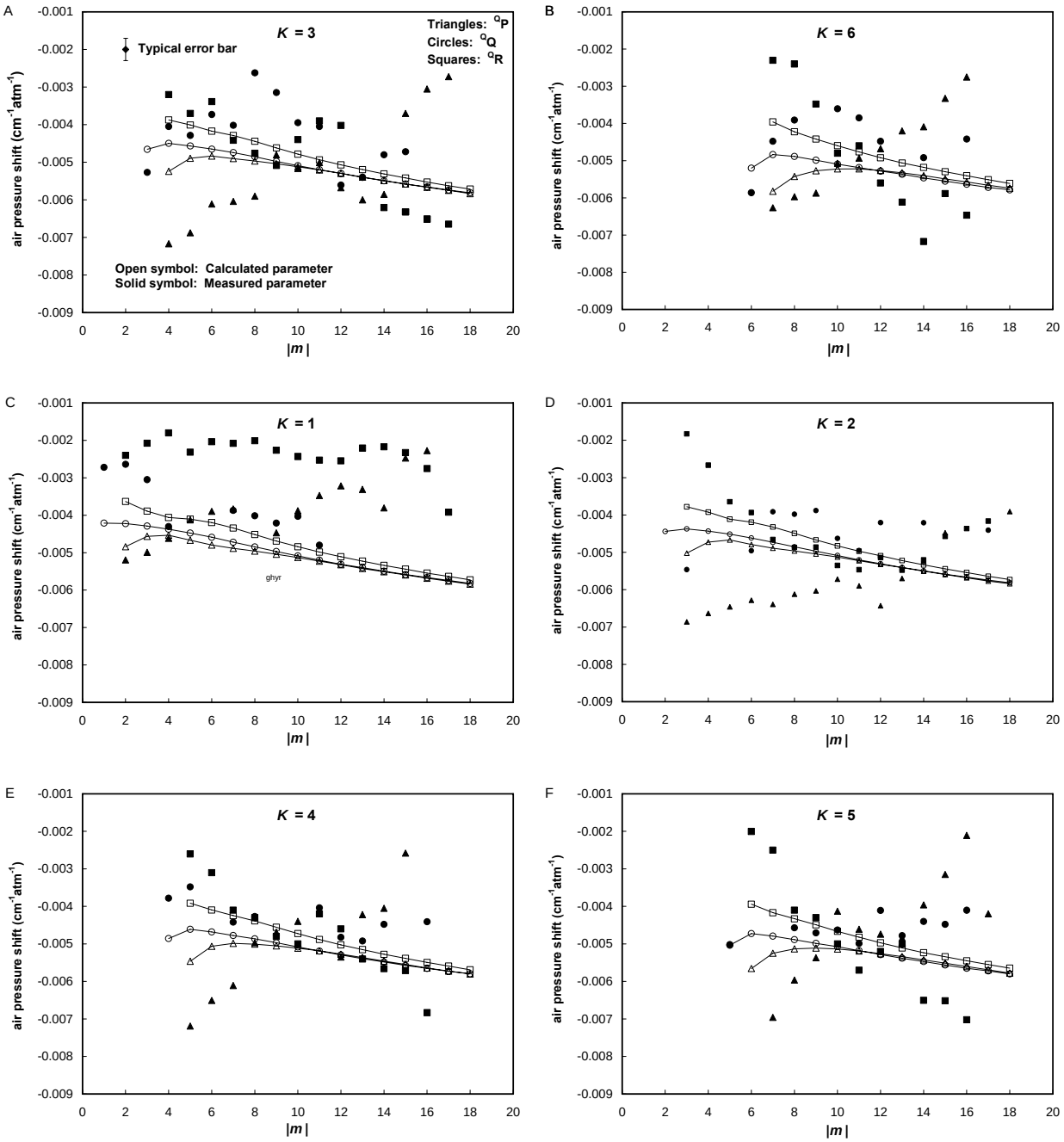
A
K = 3
Triangles: ᴼP
Circles: ᴼQ
Squares: ᴼR
Typical error bar
Open symbol: Calculated parameter
Solid symbol: Measured parameter
B
K = 6
C
K = 1
ghyr
D
K = 2
E
K = 4
F
K = 5
air pressure shift (cm-1atm-1)
|m|

Figure 8

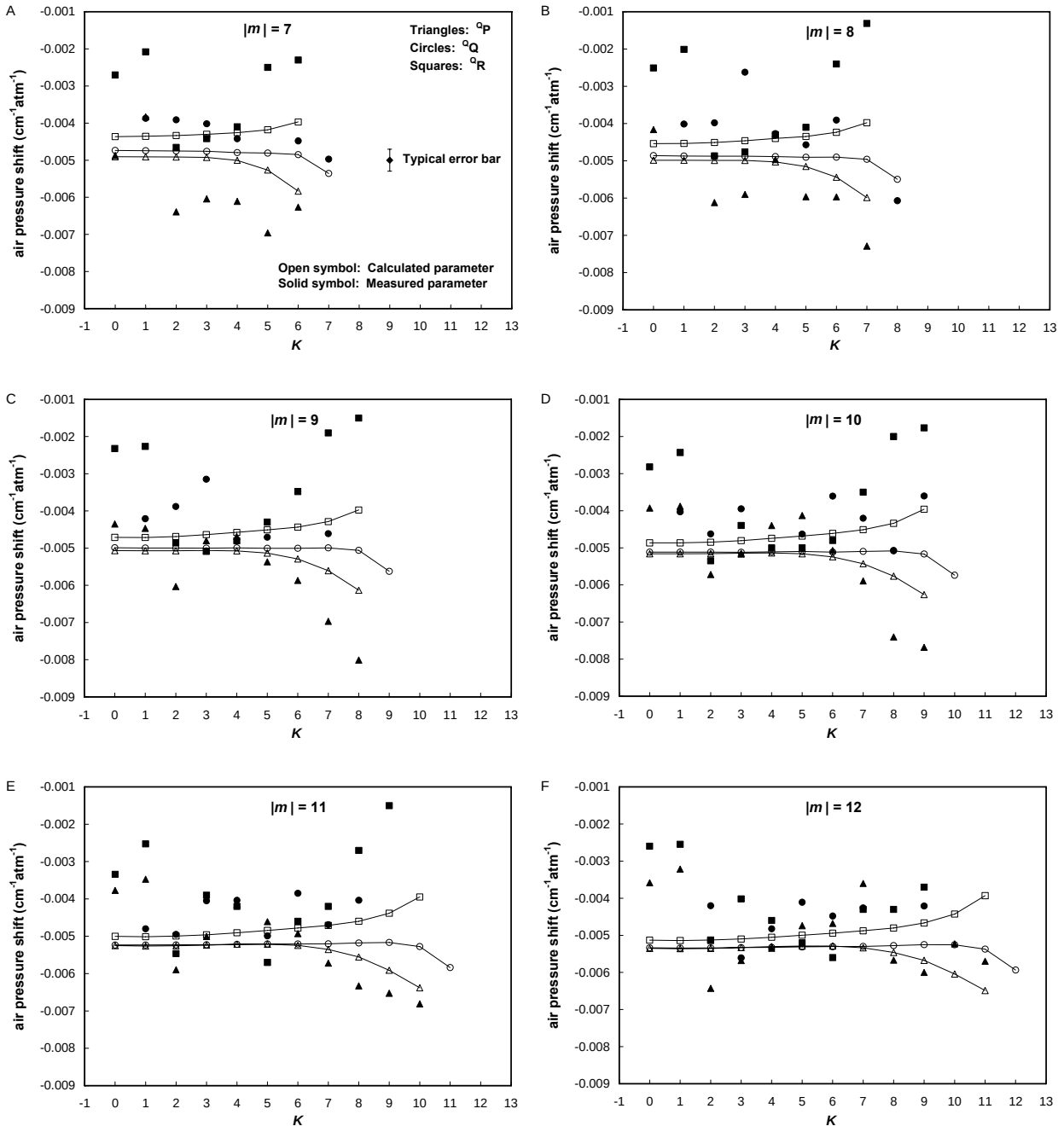
A
|m| = 7
Triangles: QP
Circles: QQ
Squares: QR
Typical error bar
Open symbol: Calculated parameter
Solid symbol: Measured parameter
B
|m| = 8
C
|m| = 9
D
|m| = 10
E
|m| = 11
F
|m| = 12
air pressure shift (cm-1atm-1)
K

Table 1

Temperature (K)	Broadening Gas	$^{12}CH_3D$ Volume Mixing Ratio	Path (cm)	Presssure (10^{-2} atm)
296.05	Air	~0.0109	25.0	13.4671
295.50	Air	~0.0109	25.0	19.8092
296.15	Air	~0.0109	25.0	26.6645
296.50	Air	~0.0109	25.0	52.8553
296.15	Air	~0.0109	150.0	13.4408
295.95	Air	~0.0109	150.0	26.4539
295.85	Air	~0.0109	150.0	39.4803
295.70	Air	~0.0109	150.0	52.6184

Note: 1atm = 101.325 kPa

Table 2

Position[ab]	J'	K'	N'	J''	K''	N''	Assignment	Measured γ(air)[ac]	Measured δ(air)[ad]	Calculated γ(air)[e]	Calculated δ(air)[e]
2184.43529(6)	1	0	A2	2	0	A1	QP(2,0,A1)	0.0665(16)	-0.0063(3)	0.0708	-0.0046
2176.50978(5)	2	0	A1	3	0	A2	QP(3,0,A2)	0.0657(14)	-0.0057(3)	0.0702	-0.0045
2168.50353(3)	3	0	A2	4	0	A1	QP(4,0,A1)	0.0656(6)	-0.0052(1)	0.0694	-0.0045
2160.41748(2)	4	0	A1	5	0	A2	QP(5,0,A2)	0.0647(6)	-0.0048(2)	0.0682	-0.0047
2152.25173(1)	5	0	A2	6	0	A1	QP(6,0,A1)	0.0640(10)	-0.0049(2)	0.0668	-0.0048
2144.00738(7)	6	0	A1	7	0	A2	QP(7,0,A2)	0.0622(6)	-0.0049(2)	0.0652	-0.0049
2135.68462(6)	7	0	A2	8	0	A1	QP(8,0,A1)	0.0629(14)	-0.0042(3)	0.0634	-0.0050
2127.28394(6)	8	0	A1	9	0	A2	QP(9,0,A2)	0.0621(6)	-0.0044(2)	0.0616	-0.0051
2118.80564(3)	9	0	A2	10	0	A1	QP(10,0,A1)	0.0614(6)	-0.0039(2)	0.0596	-0.0052
2110.24929(4)	10	0	A1	11	0	A2	QP(11,0,A2)	0.0609(6)	-0.0038(1)	0.0577	-0.0053
2101.61455(7)	11	0	A2	12	0	A1	QP(12,0,A1)	0.0595(8)	-0.0036(2)	0.0556	-0.0054
2092.90072(5)	12	0	A1	13	0	A2	QP(13,0,A2)	0.0597(4)	-0.0044(2)	0.0537	-0.0055
2084.10665(7)	13	0	A2	14	0	A1	QP(14,0,A1)	0.0557(14)	-0.0032(2)	0.0515	-0.0055
2075.23223(2)	14	0	A1	15	0	A2	QP(15,0,A2)	0.0559(18)	-0.0031(1)	0.0495	-0.0056
2066.27352(2)	15	0	A2	16	0	A1	QP(16,0,A1)	0.0526(8)		0.0474	-0.0057
2057.22871(4)	16	0	A1	17	0	A2	QP(17,0,A2)	0.0594(6)		0.0453	-0.0058
2048.09515(3)	17	0	A2	18	0	A1	QP(18,0,A1)	0.0525(4)		0.0431	-0.0059
2184.47226(4)	1	1	E	2	1	E	QP(2,1,E)	0.0681(10)	-0.0052(3)	0.0704	-0.0049
2176.54743(3)	2	1	E	3	1	E	QP(3,1,E)	0.0635(16)	-0.0050(3)	0.0704	-0.0046
2168.54072(5)	3	1	E	4	1	E	QP(4,1,E)	0.0655(6)	-0.0046(2)	0.0694	-0.0046
2160.45487(5)	4	1	E	5	1	E	QP(5,1,E)	0.0642(6)	-0.0041(2)	0.0683	-0.0047
2152.28991(3)	5	1	E	6	1	E	QP(6,1,E)	0.0642(6)	-0.0039(2)	0.0669	-0.0048
2144.04595(2)	6	1	E	7	1	E	QP(7,1,E)	0.0631(4)	-0.0038(1)	0.0653	-0.0049
2127.32383(4)	8	1	E	9	1	E	QP(9,1,E)	0.0626(8)	-0.0045(3)	0.0616	-0.0051
2118.84603(3)	9	1	E	10	1	E	QP(10,1,E)	0.062(12)	-0.0039(4)	0.0597	-0.0052
2110.29034(7)	10	1	E	11	1	E	QP(11,1,E)	0.059(10)	-0.0035(3)	0.0578	-0.0053
2101.65650(2)	11	1	E	12	1	E	QP(12,1,E)	0.0602(4)	-0.0032(3)	0.0558	-0.0054
2092.94322(2)	12	1	E	13	1	E	QP(13,1,E)	0.0600(10)	-0.0033(3)	0.0538	-0.0055
2084.15007(5)	13	1	E	14	1	E	QP(14,1,E)	0.0556(4)	-0.0038(3)	0.0517	-0.0056
2075.27502(7)	14	1	E	15	1	E	QP(15,1,E)	0.0582(4)	-0.0025(3)	0.0496	-0.0056
2066.31643(3)	15	1	E	16	1	E	QP(16,1,E)	0.0572(8)	-0.0023(3)	0.0475	-0.0057
2057.27208(6)	16	1	E	17	1	E	QP(17,1,E)	0.0582(14)		0.0454	-0.0058
2048.13866(5)	17	1	E	18	1	E	QP(18,1,E)	0.0526(8)		0.0432	-0.0059
2176.66331(8)	2	2	E	3	2	E	QP(3,2,E)	0.0697(14)	-0.0069(1)	0.068	-0.005
2168.65792(2)	3	2	E	4	2	E	QP(4,2,E)	0.0661(18)	-0.0066(2)	0.0692	-0.0047
2160.57361(5)	4	2	E	5	2	E	QP(5,2,E)	0.0642(18)	-0.0065(3)	0.0682	-0.0047
2152.40921(4)	5	2	E	6	2	E	QP(6,2,E)	0.0623(14)	-0.0063(3)	0.067	-0.0048
2144.16620(6)	6	2	E	7	2	E	QP(7,2,E)	0.0611(8)	-0.0064(2)	0.0655	-0.0049
2135.84478(2)	7	2	E	8	2	E	QP(8,2,E)	0.0609(8)	-0.0061(3)	0.0638	-0.005
2127.44604(2)	8	2	E	9	2	E	QP(9,2,E)	0.0603(10)	-0.0060(3)	0.062	-0.0051
2118.96912(3)	9	2	E	10	2	E	QP(10,2,E)	0.0591(6)	-0.0057(3)	0.06	-0.0052
2110.41506(2)	10	2	E	11	2	E	QP(11,2,E)	0.0580(14)	-0.0059(3)	0.0581	-0.0053
2101.78124(3)	11	2	E	12	2	E	QP(12,2,E)	0.0582(4)	-0.0064(3)	0.0561	-0.0054
2093.06868(2)	12	2	E	13	2	E	QP(13,2,E)	0.0571(16)	-0.0057(3)	0.0541	-0.0054
2084.27640(8)	13	2	E	14	2	E	QP(14,2,E)	0.0563(16)	-0.0052(4)	0.0521	-0.0055
2075.40264(5)	14	2	E	15	2	E	QP(15,2,E)	0.0567(14)	-0.0045(1)	0.0499	-0.0056
2066.44524(6)	15	2	E	16	2	E	QP(16,2,E)	0.0563(16)		0.0479	-0.0057

2057.40177(5)	16	2	E	17	2	E	QP(17,2,E)	0.0520(16)		0.0457	-0.0058
2048.26881(2)	17	2	E	18	2	E	QP(18,2,E)	0.0575(16)	-0.0039(4)	0.0436	-0.0059
2168.85222(6)	3	3	A1	4	3	A2	QP(4,3,A2)	0.0692(6)	-0.0072(3)	0.0657	-0.0053
2160.76868(2)	4	3	A1	5	3	A2	QP(5,3,A2)	0.0654(16)	-0.0069(3)	0.0675	-0.0049
2152.60562(6)	5	3	A2	6	3	A1	QP(6,3,A1)	0.0618(14)	-0.0061(3)	0.0668	-0.0049
2144.36466(6)	6	3	A1	7	3	A2	QP(7,3,A2)	0.0589(16)	-0.0060(3)	0.0657	-0.0049
2136.04509(4)	7	3	A2	8	3	A1	QP(8,3,A1)	0.0595(16)	-0.0059(2)	0.0641	-0.005
2127.64827(7)	8	3	A1	9	3	A2	QP(9,3,A2)	0.0552(14)	-0.0048(3)	0.0624	-0.0051
2119.17287(3)	9	3	A2	10	3	A1	QP(10,3,A1)	0.0576(14)	-0.0052(4)	0.0605	-0.0052
2110.62015(6)	10	3	A1	11	3	A2	QP(11,3,A2)	0.0538(6)	-0.0050(3)	0.0586	-0.0052
2101.98891(7)	11	3	A2	12	3	A1	QP(12,3,A1)	0.0542(14)	-0.0057(3)	0.0566	-0.0053
2093.27799(2)	12	3	A1	13	3	A2	QP(13,3,A2)	0.0575(14)	-0.0061(3)	0.0547	-0.0054
2084.48817(2)	13	3	A2	14	3	A1	QP(14,3,A1)	0.0555(10)	-0.0059(3)	0.0526	-0.0055
2075.61555(6)	14	3	A2	15	3	A1	QP(15,3,A1)	0.0549(11)	-0.0037(3)	0.0505	-0.0056
2066.66246(7)	15	3	A2	16	3	A1	QP(16,3,A1)	0.0378(14)	-0.0031(3)	0.0484	-0.0057
2057.61261(4)	16	3	A1	17	3	A2	QP(17,3,A2)	0.0535(16)	-0.0027(3)	0.0463	-0.0058
2057.62223(7)	16	3	A2	17	3	A1	QP(17,3,A1)	0.0535(16)	-0.0027(3)	0.0463	-0.0058
2048.49245(4)	17	3	A1	18	3	A2	QP(18,3,A2)	0.0404(14)		0.0441	-0.0059
2048.47792(5)	17	3	A2	18	3	A1	QP(18,3,A1)	0.0404(14)		0.0441	-0.0059
2161.04144(2)	4	4	E	5	4	E	QP(5,4,E)	0.0701(14)	-0.0072(3)	0.0637	-0.0055
2152.88105(5)	5	4	E	6	4	E	QP(6,4,E)	0.0655(8)	-0.0065(4)	0.0656	-0.0051
2144.64233(8)	6	4	E	7	4	E	QP(7,4,E)	0.0620(16)	-0.0061(3)	0.0654	-0.005
2136.32552(3)	7	4	E	8	4	E	QP(8,4,E)	0.0590(11)	-0.0050(4)	0.0642	-0.005
2127.93088(1)	8	4	E	9	4	E	QP(9,4,E)	0.0579(15)	-0.0047(1)	0.0627	-0.0051
2119.45842(3)	9	4	E	10	4	E	QP(10,4,E)	0.0551(14)	-0.0044(3)	0.061	-0.0051
2110.90804(4)	10	4	E	11	4	E	QP(11,4,E)	0.0565(14)	-0.0042(3)	0.0592	-0.0052
2102.27921(1)	11	4	E	12	4	E	QP(12,4,E)	0.0551(14)	-0.0054(2)	0.0572	-0.0053
2093.57146(2)	12	4	E	13	4	E	QP(13,4,E)	0.0526(14)	-0.0042(3)	0.0553	-0.0054
2084.78252(3)	13	4	E	14	4	E	QP(14,4,E)	0.0536(16)	-0.0041(2)	0.0533	-0.0055
2075.91330(7)	14	4	E	15	4	E	QP(15,4,E)	0.0532(14)	-0.0026(3)	0.0512	-0.0056
2066.95928(5)	15	4	E	16	4	E	QP(16,4,E)	0.0526(14)		0.0491	-0.0057
2057.91856(7)	16	4	E	17	4	E	QP(17,4,E)	0.0543(14)		0.047	-0.0058
2048.78746(3)	17	4	E	18	4	E	QP(18,4,E)	0.0565(14)		0.0449	-0.0058
2144.9982(8)	6	5	E	7	5	E	QP(7,5,E)	0.0642(14)	-0.0070(3)	0.0638	-0.0053
2136.68426(4)	7	5	E	8	5	E	QP(8,5,E)	0.0607(14)	-0.0060(4)	0.0637	-0.0052
2128.29327(5)	8	5	E	9	5	E	QP(9,5,E)	0.0576(14)	-0.0054(2)	0.0627	-0.0051
2119.82393(8)	9	5	E	10	5	E	QP(10,5,E)	0.0551(14)	-0.0041(2)	0.0612	-0.0052
2111.27717(5)	10	5	E	11	5	E	QP(11,5,E)	0.0529(16)	-0.0046(2)	0.0596	-0.0052
2102.65192(5)	11	5	E	12	5	E	QP(12,5,E)	0.0516(14)	-0.0047(3)	0.0578	-0.0053
2093.94700(4)	12	5	E	13	5	E	QP(13,5,E)	0.0519(16)	-0.0048(3)	0.0559	-0.0054
2085.16193(7)	13	5	E	14	5	E	QP(14,5,E)	0.0517(12)	-0.0040(3)	0.054	-0.0055
2076.29476(8)	14	5	E	15	5	E	QP(15,5,E)	0.0501(16)	-0.0032(4)	0.052	-0.0056
2067.34333(6)	15	5	E	16	5	E	QP(16,5,E)	0.0505(16)	-0.0021(3)	0.05	-0.0056
2058.30412(5)	16	5	E	17	5	E	QP(17,5,E)	0.0507(16)	-0.0042(3)	0.0478	-0.0057
2049.17417(7)	17	5	E	18	5	E	QP(18,5,E)	0.0568(16)		0.0458	-0.0058
2145.43180(2)	6	6	A1	7	6	A2	QP(7,6,A2)	0.0662(16)	-0.0063(3)	0.0602	-0.0058
2137.12185(4)	7	6	A1	8	6	A2	QP(8,6,A2)	0.0620(16)	-0.0060(3)	0.062	-0.0054
2128.73466(7)	8	6	A1	9	6	A2	QP(9,6,A2)	0.0583(16)	-0.0059(3)	0.062	-0.0053
2120.26963(4)	9	6	A2	10	6	A1	QP(10,6,A1)	0.0556(16)	-0.0051(4)	0.0611	-0.0052
2111.72658(4)	10	6	A2	11	6	A1	QP(11,6,A1)	0.0525(16)	-0.0049(3)	0.0598	-0.0052
2103.10524(7)	11	6	A2	12	6	A1	QP(12,6,A1)	0.0510(14)	-0.0047(3)	0.0582	-0.0053

2094.40416(6)	12	6	A2	13	6	A1	QP(13,6,A1)	0.0498(4)	-0.0042(2)	0.0565	-0.0054
2085.62253(5)	13	6	A1	14	6	A2	QP(14,6,A2)	0.0487(14)	-0.0041(3)	0.0546	-0.0054
2076.75809(2)	14	6	A2	15	6	A1	QP(15,6,A1)	0.0499(14)	-0.0033(2)	0.0528	-0.0055
2067.80915(6)	15	6	A1	16	6	A2	QP(16,6,A2)	0.048(14)	-0.0028(3)	0.0507	-0.0056
2058.77181(5)	16	6	A1	17	6	A2	QP(17,6,A2)	0.0489(4)		0.0487	-0.0057
2049.64221(3)	17	6	A1	18	6	A2	QP(18,6,A2)	0.0455(16)		0.0467	-0.0058
2137.63696(1)	7	7	E	8	7	E	QP(8,7,E)	0.0624(16)	-0.0073(4)	0.0588	-0.006
2129.25417(2)	8	7	E	9	7	E	QP(9,7,E)	0.0607(6)	-0.0070(4)	0.0603	-0.0056
2120.79364(5)	9	7	E	10	7	E	QP(10,7,E)	0.0569(14)	-0.0059(4)	0.0603	-0.0054
2112.25456(6)	10	7	E	11	7	E	QP(11,7,E)	0.0543(16)	-0.0057(3)	0.0595	-0.0054
2103.63733(1)	11	7	E	12	7	E	QP(12,7,E)	0.0506(10)	-0.0036(3)	0.0583	-0.0053
2094.93984(7)	12	7	E	13	7	E	QP(13,7,E)	0.0492(16)	-0.0041(3)	0.0567	-0.0054
2086.16171(3)	13	7	E	14	7	E	QP(14,7,E)	0.0485(16)	-0.0032(4)	0.0551	-0.0054
2077.29957(4)	14	7	E	15	7	E	QP(15,7,E)	0.0442(6)	-0.0037(3)	0.0533	-0.0055
2050.17884(7)	17	7	E	18	7	E	QP(18,7,E)	0.0383(12)	-0.0039(1)	0.0475	-0.0057
2129.85035(3)	8	8	E	9	8	E	QP(9,8,E)	0.0623(14)	-0.0080(2)	0.0573	-0.0061
2121.39287(4)	9	8	E	10	8	E	QP(10,8,E)	0.0567(6)	-0.0074(3)	0.0585	-0.0058
2112.85704(6)	10	8	E	11	8	E	QP(11,8,E)	0.0528(16)	-0.0063(2)	0.0585	-0.0056
2104.24083(2)	11	8	E	12	8	E	QP(12,8,E)	0.0512(18)	-0.0057(4)	0.0578	-0.0055
2095.54313(3)	12	8	E	13	8	E	QP(13,8,E)	0.048(12)	-0.0054(3)	0.0566	-0.0054
2086.76099(5)	13	8	E	14	8	E	QP(14,8,E)	0.0454(12)	-0.0051(3)	0.0553	-0.0055
2077.89097(3)	14	8	E	15	8	E	QP(15,8,E)	0.0451(2)	-0.0049(4)	0.0537	-0.0055
2068.92721(5)	15	8	E	16	8	E	QP(16,8,E)	0.0474(18)	-0.0042(3)	0.052	-0.0056
2050.68102(7)	17	8	E	18	8	E	QP(18,8,E)	0.0381(16)		0.0483	-0.0057
2122.01349(4)	9	9	A1	10	9	A2	QP(10,9,A2)	0.0616(2)	-0.0077(4)	0.0559	-0.0063
2113.31990(1)	10	9	A2	11	9	A1	QP(11,9,A1)	0.0562(14)	-0.0065(3)	0.0569	-0.0059
2105.49242(2)	11	9	A2	12	9	A1	QP(12,9,A1)	0.0515(0)	-0.0060(2)	0.0568	-0.0057
2096.65342(8)	12	9	A2	13	9	A1	QP(13,9,A1)	0.0488(16)	-0.0038(2)	0.056	-0.0056
2087.83144(5)	13	9	A2	14	9	A1	QP(14,9,A1)	0.0461(16)	-0.0036(2)	0.055	-0.0055
2078.96224(6)	14	9	A2	15	9	A1	QP(15,9,A1)	0.0449(16)	-0.0047(3)	0.0537	-0.0055
2070.02322(2)	15	9	A2	16	9	A1	QP(16,9,A1)	0.0427(18)	-0.0047(3)	0.0522	-0.0056
2060.99774(1)	16	9	A1	17	9	A2	QP(17,9,A2)	0.0403(16)		0.0506	-0.0056
2061.00202(2)	16	9	A2	17	9	A1	QP(17,9,A1)	0.0403(16)		0.0506	-0.0056
2051.87889(4)	17	9	A1	18	9	A2	QP(18,9,A2)	0.0448(12)		0.0489	-0.0057
2051.91086(1)	17	9	A2	18	9	A1	QP(18,9,A1)	0.0448(12)		0.0489	-0.0057
2114.33654(6)	10	10	E	11	10	E	QP(11,10,E)	0.0601(14)	-0.0068(3)	0.0545	-0.0064
2105.75848(1)	11	10	E	12	10	E	QP(12,10,E)	0.0531(14)	-0.0052(4)	0.0553	-0.006
2097.10256(1)	12	10	E	13	10	E	QP(13,10,E)	0.0498(4)	-0.0049(1)	0.055	-0.0058
2088.36700(3)	13	10	E	14	10	E	QP(14,10,E)	0.0511(16)	-0.0048(3)	0.0543	-0.0057
2079.54940(3)	14	10	E	15	10	E	QP(15,10,E)	0.0454(16)	-0.0031(4)	0.0533	-0.0056
2070.64706(8)	15	10	E	16	10	E	QP(16,10,E)	0.0449(18)		0.0521	-0.0056
2061.65610(2)	16	10	E	17	10	E	QP(17,10,E)	0.0385(16)	-0.0045(4)	0.0507	-0.0057
2052.57215(4)	17	10	E	18	10	E	QP(18,10,E)	0.0429(6)		0.0492	-0.0057
2106.59120(2)	11	11	E	12	11	E	QP(12,11,E)	0.0528(10)	-0.0057(3)	0.0532	-0.0065
2097.94340(3)	12	11	E	13	11	E	QP(13,11,E)	0.0511(8)	-0.0052(4)	0.0537	-0.0062
2089.21599(8)	13	11	E	14	11	E	QP(14,11,E)	0.0508(6)	-0.0039(3)	0.0532	-0.0059
2071.51391(6)	15	11	E	16	11	E	QP(16,11,E)	0.0426(14)	-0.0040(3)	0.0516	-0.0057
2062.53151(3)	16	11	E	17	11	E	QP(17,11,E)	0.0405(14)	-0.0039(2)	0.0505	-0.0057
2053.45483(1)	17	11	E	18	11	E	QP(18,11,E)	0.0610(14)	-0.0039(3)	0.0492	-0.0057
2072.47669(3)	15	12	A2	16	12	A1	QP(16,12,A1)	0.0439(10)		0.0507	-0.0059
2063.50675(7)	16	12	A2	17	12	A1	QP(17,12,A1)	0.0453(16)	-0.0041(3)	0.0498	-0.0058

2054.44137(7)	17	12	A1	18	12	A2	QP(18,12,A2)	0.0341(4)		0.0487	-0.0058
2199.99135(4)	1	1	E	1	1	E	QQ(1,1,E)	0.0666(16)	-0.0027(3)	0.0707	-0.0042
2199.82235(4)	2	1	E	2	1	E	QQ(2,1,E)	0.0660(10)	-0.0026(3)	0.0705	-0.0042
2199.56873(6)	3	1	E	3	1	E	QQ(3,1,E)	0.0591(8)	-0.0031(3)	0.0694	-0.0043
2199.22905(7)	4	1	E	4	1	E	QQ(4,1,E)	0.0584(10)	-0.0043(3)	0.0683	-0.0044
2198.29571(5)	6	1	E	6	1	E	QQ(6,1,E)	0.0561(8)		0.0655	-0.0046
2197.69839(4)	7	1	E	7	1	E	QQ(7,1,E)	0.0640(12)	-0.0039(3)	0.0637	-0.0047
2197.01249(7)	8	1	E	8	1	E	QQ(8,1,E)	0.0637(10)	-0.0040(3)	0.0618	-0.0049
2196.23834(6)	9	1	E	9	1	E	QQ(9,1,E)	0.0650(6)	-0.0042(4)	0.0599	-0.005
2195.37335(2)	10	1	E	10	1	E	QQ(10,1,E)	0.0512(6)	-0.0040(4)	0.0579	-0.0051
2194.41671(2)	11	1	E	11	1	E	QQ(11,1,E)	0.0568(6)	-0.0048(3)	0.0558	-0.0052
2189.62513(7)	15	1	E	15	1	E	QQ(15,1,E)	0.0492(4)		0.0473	-0.0056
2199.93605(7)	2	2	E	2	2	E	QQ(2,2,E)	0.0666(6)		0.0672	-0.0045
2199.68208(3)	3	2	E	3	2	E	QQ(3,2,E)	0.0634(8)	-0.0055(3)	0.0683	-0.0044
2198.40956(4)	6	2	E	6	2	E	QQ(6,2,E)	0.0631(6)	-0.0050(4)	0.0651	-0.0046
2197.81181(8)	7	2	E	7	2	E	QQ(7,2,E)	0.0630(4)	-0.0039(3)	0.0635	-0.0048
2197.12740(1)	8	2	E	8	2	E	QQ(8,2,E)	0.0603(12)	-0.0040(3)	0.0618	-0.0049
2196.35291(3)	9	2	E	9	2	E	QQ(9,2,E)	0.0606(10)	-0.0039(4)	0.0599	-0.005
2195.48900(7)	10	2	E	10	2	E	QQ(10,2,E)	0.0586(10)	-0.0046(3)	0.0579	-0.0051
2194.53259(2)	11	2	E	11	2	E	QQ(11,2,E)	0.0591(8)	-0.0050(3)	0.0559	-0.0052
2193.48199(7)	12	2	E	12	2	E	QQ(12,2,E)	0.0541(6)	-0.0042(3)	0.0539	-0.0053
2191.09024(6)	14	2	E	14	2	E	QQ(14,2,E)	0.0524(14)	-0.0042(3)	0.0497	-0.0055
2186.72660(3)	17	2	E	17	2	E	QQ(17,2,E)	0.0478(14)	-0.0044(3)	0.0431	-0.0058
2181.32262(5)	20	2	E	20	2	E	QQ(20,2,E)	0.0565(6)		0.0363	-0.006
2199.87131(5)	3	3	A1	3	3	A2	QQ(3,3,A2)	0.0641(8)	-0.0053(1)	0.0637	-0.0047
2199.53369(6)	4	3	A1	4	3	A2	QQ(4,3,A2)	0.0641(6)	-0.0041(3)	0.0666	-0.0045
2199.10889(7)	5	3	A2	5	3	A1	QQ(5,3,A1)	0.0637(4)	-0.0043(3)	0.0657	-0.0046
2198.59957(3)	6	3	A1	6	3	A2	QQ(6,3,A2)	0.0617(10)	-0.0037(3)	0.0646	-0.0047
2198.00288(6)	7	3	A2	7	3	A1	QQ(7,3,A1)	0.0626(10)	-0.0040(1)	0.0633	-0.0048
2197.31815(6)	8	3	A2	8	3	A1	QQ(8,3,A1)	0.0596(10)	-0.0026(4)	0.0616	-0.0049
2196.54523(7)	9	3	A2	9	3	A1	QQ(9,3,A1)	0.0588(8)	-0.0032(3)	0.0598	-0.005
2195.67913(8)	10	3	A2	10	3	A1	QQ(10,3,A1)	0.0608(8)	-0.0040(3)	0.058	-0.0051
2194.72586(6)	11	3	A1	11	3	A2	QQ(11,3,A2)	0.0597(6)	-0.0041(3)	0.056	-0.0052
2193.67458(4)	12	3	A1	12	3	A2	QQ(12,3,A2)	0.0574(4)	-0.0056(4)	0.054	-0.0053
2192.52959(5)	13	3	A2	13	3	A1	QQ(13,3,A1)	0.0577(8)	-0.0054(3)	0.052	-0.0054
2191.28476(7)	14	3	A2	14	3	A1	QQ(14,3,A1)	0.0526(12)	-0.0048(3)	0.0499	-0.0055
2189.94137(7)	15	3	A1	15	3	A2	QQ(15,3,A2)	0.0497(6)	-0.0047(3)	0.0478	-0.0056
2181.53945(4)	20	3	A2	20	3	A1	QQ(20,3,A1)	0.0724(14)		0.0367	-0.006
2181.48860(8)	20	3	A1	20	3	A2	QQ(20,3,A2)	0.0836(10)		0.0367	-0.006
2199.79569(6)	4	4	E	4	4	E	QQ(4,4,E)	0.0599(10)	-0.0038(4)	0.0603	-0.0049
2199.37267(3)	5	4	E	5	4	E	QQ(5,4,E)	0.0643(10)	-0.0035(3)	0.0649	-0.0046
2198.26778(2)	7	4	E	7	4	E	QQ(7,4,E)	0.0609(4)	-0.0044(3)	0.0629	-0.0048
2197.58512(7)	8	4	E	8	4	E	QQ(8,4,E)	0.0588(8)	-0.0043(3)	0.0614	-0.0049
2194.99493(8)	11	4	E	11	4	E	QQ(11,4,E)	0.0547(10)	-0.0040(4)	0.0561	-0.0052
2193.94617(6)	12	4	E	12	4	E	QQ(12,4,E)	0.0555(8)	-0.0048(3)	0.0541	-0.0053
2192.80120(3)	13	4	E	13	4	E	QQ(13,4,E)	0.0530(14)	-0.0049(3)	0.0522	-0.0054
2191.55665(2)	14	4	E	14	4	E	QQ(14,4,E)	0.0518(16)	-0.0045(3)	0.0501	-0.0055
2188.75775(6)	16	4	E	16	4	E	QQ(16,4,E)	0.0398(2)	-0.0044(3)	0.0459	-0.0057
2187.19394(4)	17	4	E	17	4	E	QQ(17,4,E)	0.0422(10)		0.0438	-0.0058
2199.71317(3)	5	5	E	5	5	E	QQ(5,5,E)	0.0555(6)	-0.0050(3)	0.0568	-0.0051
2197.92767(5)	8	5	E	8	5	E	QQ(8,5,E)	0.0571(4)	-0.0046(3)	0.0613	-0.0049

2197.15656(7)	9	5	E	9	5	E	QQ(9,5,E)	0.0556(6)	-0.0047(3)	0.0598	-0.005
2196.29437(4)	10	5	E	10	5	E	QQ(10,5,E)	0.0547(8)	-0.0046(3)	0.058	-0.0051
2195.34090(7)	11	5	E	11	5	E	QQ(11,5,E)	0.0545(6)	-0.0050(4)	0.0562	-0.0052
2194.29336(5)	12	5	E	12	5	E	QQ(12,5,E)	0.0525(12)	-0.0041(3)	0.0543	-0.0053
2193.14909(4)	13	5	E	13	5	E	QQ(13,5,E)	0.0527(16)	-0.0048(3)	0.0524	-0.0054
2191.90522(3)	14	5	E	14	5	E	QQ(14,5,E)	0.0523(16)	-0.0044(3)	0.0504	-0.0055
2190.55964(5)	15	5	E	15	5	E	QQ(15,5,E)	0.0519(10)	-0.0045(4)	0.0484	-0.0056
2189.10671(2)	16	5	E	16	5	E	QQ(16,5,E)	0.0641(12)	-0.0041(3)	0.0463	-0.0057
2187.54251(3)	17	5	E	17	5	E	QQ(17,5,E)	0.0417(8)		0.0443	-0.0058
2199.61867(6)	6	6	A1	6	6	A2	QQ(6,6,A2)	0.0520(6)	-0.0059(3)	0.0535	-0.0052
2199.02531(4)	7	6	A2	7	6	A1	QQ(7,6,A1)	0.0597(8)	-0.0045(4)	0.0615	-0.0049
2198.34473(1)	8	6	A1	8	6	A2	QQ(8,6,A2)	0.0593(8)	-0.0039(4)	0.0612	-0.0049
2196.71403(1)	10	6	A2	10	6	A1	QQ(10,6,A1)	0.0549(6)	-0.0036(4)	0.0581	-0.0051
2195.76214(3)	11	6	A1	11	6	A2	QQ(11,6,A2)	0.0528(14)	-0.0039(3)	0.0563	-0.0052
2194.71596(3)	12	6	A1	12	6	A2	QQ(12,6,A2)	0.0509(14)	-0.0045(3)	0.0545	-0.0053
2192.32972(2)	14	6	A1	14	6	A2	QQ(14,6,A2)	0.0495(16)	-0.0049(4)	0.0506	-0.0055
2189.52889(5)	16	6	A2	16	6	A1	QQ(16,6,A1)	0.0441(14)	-0.0044(3)	0.0467	-0.0057
2187.96313(4)	17	6	A2	17	6	A1	QQ(17,6,A1)	0.0463(14)		0.0447	-0.0058
2199.51407(1)	7	7	E	7	7	E	QQ(7,7,E)	0.0454(14)	-0.0050(3)	0.0502	-0.0054
2198.06568(7)	9	7	E	9	7	E	QQ(9,7,E)	0.0563(10)	-0.0046(4)	0.0597	-0.005
2197.20767(2)	10	7	E	10	7	E	QQ(10,7,E)	0.0537(6)	-0.0042(3)	0.0584	-0.0051
2196.25599(7)	11	7	E	11	7	E	QQ(11,7,E)	0.0516(10)	-0.0047(3)	0.0565	-0.0052
2195.20863(5)	12	7	E	12	7	E	QQ(12,7,E)	0.0498(10)	-0.0043(3)	0.0547	-0.0053
2194.06568(4)	13	7	E	13	7	E	QQ(13,7,E)	0.0469(6)	-0.0045(4)	0.0529	-0.0054
2192.82282(1)	14	7	E	14	7	E	QQ(14,7,E)	0.0450(13)	-0.0046(3)	0.0509	-0.0055
2191.47470(3)	15	7	E	15	7	E	QQ(15,7,E)	0.0502(16)	-0.0044(3)	0.049	-0.0056
2188.44420(4)	17	7	E	17	7	E	QQ(17,7,E)	0.0641(13)	-0.0046(3)	0.0451	-0.0057
2186.74826(7)	18	7	E	18	7	E	QQ(18,7,E)	0.0627(16)		0.043	-0.0058
2199.39811(6)	8	8	E	8	8	E	QQ(8,8,E)	0.0418(4)	-0.0061(3)	0.047	-0.0055
2197.76694(6)	10	8	E	10	8	E	QQ(10,8,E)	0.0541(4)	-0.0051(3)	0.0582	-0.0051
2196.81429(5)	11	8	E	11	8	E	QQ(11,8,E)	0.0512(13)	-0.0040(4)	0.0568	-0.0052
2194.61425(4)	13	8	E	13	8	E	QQ(13,8,E)	0.0467(13)	-0.0043(3)	0.0532	-0.0054
2193.35975(6)	14	8	E	14	8	E	QQ(14,8,E)	0.0451(13)		0.0513	-0.0055
2190.50496(5)	16	8	E	16	8	E	QQ(16,8,E)	0.0442(16)		0.0474	-0.0056
2187.09852(2)	18	8	E	18	8	E	QQ(18,8,E)	0.0610(14)		0.0434	-0.0058
2199.20552(6)	9	9	A1	9	9	A2	QQ(9,9,A2)	0.0388(13)		0.0438	-0.0056
2198.18541(1)	10	9	A1	10	9	A2	QQ(10,9,A2)	0.0507(16)	-0.0036(3)	0.0558	-0.0052
2196.82114(4)	12	9	A1	12	9	A2	QQ(12,9,A2)	0.0489(16)	-0.0042(3)	0.0553	-0.0053
2195.62673(6)	13	9	A2	13	9	A1	QQ(13,9,A1)	0.0467(13)	-0.0040(3)	0.0535	-0.0054
2194.36935(5)	14	9	A1	14	9	A2	QQ(14,9,A2)	0.0434(16)	-0.0046(3)	0.0516	-0.0055
2193.02207(8)	15	9	A2	15	9	A1	QQ(15,9,A1)	0.0410(2)	-0.0042(3)	0.0497	-0.0055
2188.37686(2)	18	9	A2	18	9	A1	QQ(18,9,A1)	0.0399(16)		0.0438	-0.0058
2199.14837(6)	10	10	E	10	10	E	QQ(10,10,E)	0.0344(2)		0.0409	-0.0057
2198.22409(4)	11	10	E	11	10	E	QQ(11,10,E)	0.0488(16)		0.0538	-0.0053
2196.09658(6)	13	10	E	13	10	E	QQ(13,10,E)	0.0473(16)	-0.0053(3)	0.0537	-0.0053
2194.88572(2)	14	10	E	14	10	E	QQ(14,10,E)	0.0473(13)	-0.0044(3)	0.052	-0.0054
2193.57237(2)	15	10	E	15	10	E	QQ(15,10,E)	0.0560(6)	-0.0042(3)	0.0501	-0.0055
2192.15202(2)	16	10	E	16	10	E	QQ(16,10,E)	0.0441(4)		0.0481	-0.0056
2187.17886(2)	19	10	E	19	10	E	QQ(19,10,E)	0.0640(4)		0.0422	-0.0058
2198.99481(1)	11	11	E	11	11	E	QQ(11,11,E)	0.0316(16)		0.038	-0.0058
2197.98130(2)	12	11	E	12	11	E	QQ(12,11,E)	0.0481(16)		0.0516	-0.0054

2196.87263(4)	13	11	E	13	11	E	QQ(13,11,E)	0.0464(4)	-0.0056(3)	0.0531	-0.0053
2195.66628(1)	14	11	E	14	11	E	QQ(14,11,E)	0.0410(16)	-0.0042(3)	0.0521	-0.0054
2194.35730(8)	15	11	E	15	11	E	QQ(15,11,E)	0.0438(13)	-0.0044(3)	0.0505	-0.0055
2192.94043(6)	16	11	E	16	11	E	QQ(16,11,E)	0.0354(13)	-0.0042(3)	0.0485	-0.0056
2189.75489(3)	18	11	E	18	11	E	QQ(18,11,E)	0.0206(16)		0.0446	-0.0058
2197.73048(8)	13	12	A1	13	12	A2	QQ(13,12,A2)	0.0414(2)	-0.0052(3)	0.0495	-0.0055
2196.53153(4)	14	12	A2	14	12	A1	QQ(14,12,A1)	0.0432(13)	-0.0064(3)	0.0512	-0.0054
2195.23051(5)	15	12	A1	15	12	A2	QQ(15,12,A2)	0.0427(2)	-0.0058(3)	0.0504	-0.0055
2192.29547(6)	17	12	A1	17	12	A2	QQ(17,12,A2)	0.0388(11)		0.047	-0.0056
2190.64568(3)	18	12	A1	18	12	A2	QQ(18,12,A2)	0.0406(14)		0.0451	-0.0057
2188.86058(5)	19	12	A1	19	12	A2	QQ(19,12,A2)	0.0389(8)		0.0431	-0.0058
2197.46671(2)	14	13	E	14	13	E	QQ(14,13,E)	0.0375(13)	-0.0064(3)	0.0472	-0.0056
2196.17674(3)	15	13	E	15	13	E	QQ(15,13,E)	0.0423(16)	-0.0063(3)	0.0494	-0.0055
2194.77813(1)	16	13	E	16	13	E	QQ(16,13,E)	0.0384(10)	-0.0057(3)	0.0488	-0.0055
2191.62061(4)	18	13	E	18	13	E	QQ(18,13,E)	0.0586(16)		0.0455	-0.0057
2189.83635(5)	19	13	E	19	13	E	QQ(19,13,E)	0.0797(9)		0.0435	-0.0058
2197.18868(3)	15	14	E	15	14	E	QQ(15,14,E)	0.0427(13)		0.045	-0.0057
2195.80574(7)	16	14	E	16	14	E	QQ(16,14,E)	0.0427(14)	-0.0042(4)	0.0474	-0.0056
2194.30433(4)	17	14	E	17	14	E	QQ(17,14,E)	0.0370(13)		0.047	-0.0056
2192.67016(3)	18	14	E	18	14	E	QQ(18,14,E)	0.0326(6)		0.0456	-0.0057
2188.85546(8)	20	14	E	20	14	E	QQ(20,14,E)	0.0516(10)		0.0419	-0.0058
2196.91999(3)	16	15	A1	16	15	A2	QQ(16,15,A2)	0.0343(8)		0.0427	-0.0058
2195.42515(6)	17	15	A1	17	15	A2	QQ(17,15,A2)	0.0341(11)		0.0455	-0.0057
2272.76404(7)	10	1	E	9	1	E	QR(9,1,E)	0.0629(2)	-0.0024(3)	0.0597	-0.0049
2279.49865(1)	11	1	E	10	1	E	QR(10,1,E)	0.0614(16)	-0.0025(4)	0.0578	-0.005
2286.12455(2)	12	1	E	11	1	E	QR(11,1,E)	0.0609(16)	-0.0026(3)	0.0557	-0.0051
2292.64101(4)	13	1	E	12	1	E	QR(12,1,E)	0.0592(13)	-0.0022(3)	0.0538	-0.0053
2299.04128(2)	14	1	E	13	1	E	QR(13,1,E)	0.0583(6)	-0.0022(3)	0.0517	-0.0054
2305.32294(3)	15	1	E	14	1	E	QR(14,1,E)	0.0573(8)	-0.0023(3)	0.0496	-0.0055
2311.48059(6)	16	1	E	15	1	E	QR(15,1,E)	0.0564(4)	-0.0028(4)	0.0475	-0.0056
2317.51065(2)	17	1	E	16	1	E	QR(16,1,E)	0.0547(16)	-0.0039(4)	0.0454	-0.0057
2222.95472(8)	3	2	E	2	2	E	QR(2,2,E)	0.0702(16)	-0.0018(3)	0.068	-0.0038
2230.36765(4)	4	2	E	3	2	E	QR(3,2,E)	0.0657(4)	-0.0027(3)	0.0691	-0.0039
2237.69012(5)	5	2	E	4	2	E	QR(4,2,E)	0.0646(16)	-0.0037(3)	0.0682	-0.0041
2244.92025(1)	6	2	E	5	2	E	QR(5,2,E)	0.0623(13)	-0.0039(3)	0.067	-0.0042
2252.05626(5)	7	2	E	6	2	E	QR(6,2,E)	0.0629(13)	-0.0047(3)	0.0655	-0.0043
2259.09459(8)	8	2	E	7	2	E	QR(7,2,E)	0.0610(16)	-0.0049(3)	0.0638	-0.0045
2266.03457(2)	9	2	E	8	2	E	QR(8,2,E)	0.0602(2)	-0.0049(3)	0.0619	-0.0047
2272.87293(3)	10	2	E	9	2	E	QR(9,2,E)	0.0594(13)	-0.0054(3)	0.06	-0.0049
2279.60697(5)	11	2	E	10	2	E	QR(10,2,E)	0.0591(2)	-0.0055(3)	0.0581	-0.005
2286.23296(3)	12	2	E	11	2	E	QR(11,2,E)	0.0575(11)	-0.0051(3)	0.0561	-0.0051
2292.74831(7)	13	2	E	12	2	E	QR(12,2,E)	0.0585(14)	-0.0055(3)	0.054	-0.0053
2299.14841(1)	14	2	E	13	2	E	QR(13,2,E)	0.0564(8)	-0.0053(3)	0.052	-0.0054
2305.42989(4)	15	2	E	14	2	E	QR(14,2,E)	0.0553(13)	-0.0046(3)	0.0499	-0.0055
2311.58642(2)	16	2	E	15	2	E	QR(15,2,E)	0.0565(16)	-0.0044(4)	0.0479	-0.0056
2317.61458(6)	17	2	E	16	2	E	QR(16,2,E)	0.0479(10)	-0.0042(3)	0.0457	-0.0057
2230.55145(4)	4	3	A2	3	3	A1	QR(3,3,A1)	0.0695(16)	-0.0033(3)	0.0656	-0.0039
2237.87342(3)	5	3	A1	4	3	A2	QR(4,3,A2)	0.0663(6)	-0.0038(3)	0.0674	-0.004
2245.10241(8)	6	3	A2	5	3	A1	QR(5,3,A1)	0.0619(13)	-0.0034(1)	0.0668	-0.0042
2252.23766(2)	7	3	A2	6	3	A1	QR(6,3,A1)	0.0595(14)	-0.0044(3)	0.0656	-0.0043
2259.27541(7)	8	3	A2	7	3	A1	QR(7,3,A1)	0.0577(13)	-0.0048(3)	0.0641	-0.0045

2266.21520(4)	9	3	A2	8	3	A1	QR(8,3,A1)	0.0562(6)	-0.0051(3)	0.0623	-0.0046
2273.05274(5)	10	3	A2	9	3	A1	QR(9,3,A1)	0.0552(10)	-0.0045(3)	0.0605	-0.0048
2279.78607(2)	11	3	A2	10	3	A1	QR(10,3,A1)	0.0628(8)	-0.0040(3)	0.0586	-0.005
2286.41155(4)	12	3	A1	11	3	A2	QR(11,3,A2)	0.0583(11)	-0.0040(4)	0.0566	-0.0051
2299.32390(4)	14	3	A2	13	3	A1	QR(13,3,A1)	0.0541(13)	-0.0062(3)	0.0525	-0.0054
2305.61120(7)	15	3	A1	14	3	A2	QR(14,3,A2)	0.0562(14)	-0.0063(3)	0.0505	-0.0055
2305.60303(7)	15	3	A2	14	3	A1	QR(14,3,A1)	0.0575(16)	-0.0063(1)	0.0505	-0.0055
2311.75796(2)	16	3	A1	15	3	A2	QR(15,3,A2)	0.0542(6)	-0.0065(3)	0.0484	-0.0056
2311.76986(5)	16	3	A2	15	3	A1	QR(15,3,A1)	0.0542(6)	-0.0065(3)	0.0484	-0.0056
2317.79703(2)	17	3	A1	16	3	A2	QR(16,3,A2)	0.0572(14)	-0.0067(3)	0.0463	-0.0057
2238.12967(6)	5	4	E	4	4	E	QR(4,4,E)	0.0696(14)	-0.0026(4)	0.0636	-0.0039
2245.35752(2)	6	4	E	5	4	E	QR(5,4,E)	0.0657(10)	-0.0031(4)	0.0655	-0.0041
2252.49117(4)	7	4	E	6	4	E	QR(6,4,E)	0.0620(6)	-0.0041(4)	0.0653	-0.0043
2259.52850(4)	8	4	E	7	4	E	QR(7,4,E)	0.0598(10)	-0.0043(3)	0.0641	-0.0044
2266.46736(5)	9	4	E	8	4	E	QR(8,4,E)	0.0581(10)	-0.0048(3)	0.0627	-0.0046
2273.30407(2)	10	4	E	9	4	E	QR(9,4,E)	0.0557(6)	-0.0051(4)	0.061	-0.0047
2280.03704(4)	11	4	E	10	4	E	QR(10,4,E)	0.0548(13)	-0.0042(3)	0.0591	-0.0049
2286.66185(3)	12	4	E	11	4	E	QR(11,4,E)	0.0534(16)	-0.0046(3)	0.0572	-0.0051
2293.17562(4)	13	4	E	12	4	E	QR(12,4,E)	0.0532(13)	-0.0054(3)	0.0553	-0.0052
2299.57463(4)	14	4	E	13	4	E	QR(13,4,E)	0.0539(12)	-0.0057(3)	0.0532	-0.0053
2305.85391(3)	15	4	E	14	4	E	QR(14,4,E)	0.0518(4)	-0.0057(4)	0.0512	-0.0054
2312.00867(4)	16	4	E	15	4	E	QR(15,4,E)	0.0516(4)	-0.0068(3)	0.0491	-0.0055
2245.68405(4)	6	5	E	5	5	E	QR(5,5,E)	0.0676(13)	-0.0021(3)	0.0618	-0.004
2252.81684(8)	7	5	E	6	5	E	QR(6,5,E)	0.0640(13)	-0.0025(4)	0.0638	-0.0042
2259.85372(6)	8	5	E	7	5	E	QR(7,5,E)	0.0609(13)	-0.0041(3)	0.0636	-0.0044
2266.79008(6)	9	5	E	8	5	E	QR(8,5,E)	0.0583(16)	-0.0043(3)	0.0627	-0.0045
2273.62648(4)	10	5	E	9	5	E	QR(9,5,E)	0.0546(14)	-0.0051(3)	0.0612	-0.0047
2280.35814(5)	11	5	E	10	5	E	QR(10,5,E)	0.0530(13)	-0.0057(3)	0.0596	-0.0048
2286.98231(6)	12	5	E	11	5	E	QR(11,5,E)	0.0510(16)	-0.0052(3)	0.0578	-0.005
2293.49504(5)	13	5	E	12	5	E	QR(12,5,E)	0.0477(16)	-0.0051(4)	0.0559	-0.0051
2299.89231(3)	14	5	E	13	5	E	QR(13,5,E)	0.0515(13)	-0.0065(3)	0.054	-0.0053
2306.17004(7)	15	5	E	14	5	E	QR(14,5,E)	0.0512(16)	-0.0065(3)	0.0519	-0.0054
2312.32276(2)	16	5	E	15	5	E	QR(15,5,E)	0.0451(2)	-0.0070(1)	0.0499	-0.0055
2253.21294(4)	7	6	A1	6	6	A2	QR(6,6,A2)	0.0659(12)	-0.0023(3)	0.0602	-0.004
2260.24766(4)	8	6	A2	7	6	A1	QR(7,6,A1)	0.0626(2)	-0.0024(3)	0.0619	-0.0042
2267.18372(1)	9	6	A2	8	6	A1	QR(8,6,A1)	0.0591(12)	-0.0035(3)	0.062	-0.0044
2274.01868(1)	10	6	A2	9	6	A1	QR(9,6,A1)	0.0565(12)	-0.0048(3)	0.0611	-0.0046
2280.74872(7)	11	6	A2	10	6	A1	QR(10,6,A1)	0.0530(13)	-0.0046(3)	0.0598	-0.0048
2287.37144(6)	12	6	A2	11	6	A1	QR(11,6,A1)	0.0510(6)	-0.0056(4)	0.0582	-0.0049
2293.88286(2)	13	6	A1	12	6	A2	QR(12,6,A2)	0.0503(10)	-0.0061(3)	0.0565	-0.0051
2300.27823(2)	14	6	A1	13	6	A2	QR(13,6,A2)	0.0481(4)	-0.0072(3)	0.0546	-0.0052
2306.55373(3)	15	6	A1	14	6	A2	QR(14,6,A2)	0.0486(12)	-0.0059(1)	0.0527	-0.0053
2312.70311(5)	16	6	A1	15	6	A2	QR(15,6,A2)	0.0481(12)	-0.0065(3)	0.0507	-0.0054
2260.71206(7)	8	7	E	7	7	E	QR(7,7,E)	0.0641(4)		0.0586	-0.004
2267.64607(5)	9	7	E	8	7	E	QR(8,7,E)	0.0601(12)	-0.0019(3)	0.0602	-0.0043
2274.47886(3)	10	7	E	9	7	E	QR(9,7,E)	0.0569(13)	-0.0035(4)	0.0602	-0.0045
2281.20726(7)	11	7	E	10	7	E	QR(10,7,E)	0.0543(13)	-0.0042(4)	0.0594	-0.0047
2287.82756(4)	12	7	E	11	7	E	QR(11,7,E)	0.0499(12)	-0.0043(4)	0.0582	-0.0049
2294.33557(5)	13	7	E	12	7	E	QR(12,7,E)	0.0482(2)	-0.0041(3)	0.0567	-0.005
2300.72756(3)	14	7	E	13	7	E	QR(13,7,E)	0.0477(13)	-0.0056(3)	0.0551	-0.0052
2306.99748(7)	15	7	E	14	7	E	QR(14,7,E)	0.0456(2)	-0.0044(4)	0.0533	-0.0053

2268.17420(5)	9	8	E	8	8	E	QR(8,8,E)	0.0635(11)		0.0572	-0.004
2275.00279(2)	10	8	E	9	8	E	QR(9,8,E)	0.0588(14)	-0.0020(3)	0.0585	-0.0043
2281.72534(6)	11	8	E	10	8	E	QR(10,8,E)	0.0549(8)	-0.0027(3)	0.0584	-0.0046
2288.33770(5)	12	8	E	11	8	E	QR(11,8,E)	0.0511(13)	-0.0043(3)	0.0577	-0.0048
2294.83574(1)	13	8	E	12	8	E	QR(12,8,E)	0.0478(12)	-0.0022(4)	0.0566	-0.005
2301.21284(5)	14	8	E	13	8	E	QR(13,8,E)	0.0453(10)	-0.0059(3)	0.0553	-0.0051
2307.46083(2)	15	8	E	14	8	E	QR(14,8,E)	0.0450(12)	-0.0055(3)	0.0537	-0.0052
2313.57037(2)	16	8	E	15	8	E	QR(15,8,E)	0.0450(0)	-0.0057(4)	0.052	-0.0054
2275.37720(4)	10	9	A2	9	9	A1	QR(9,9,A1)	0.059(13)		0.0558	-0.004
2282.87966(5)	11	9	A2	10	9	A1	QR(10,9,A1)	0.0607(14)	-0.0015(3)	0.0568	-0.0044
2289.34384(8)	12	9	A2	11	9	A1	QR(11,9,A1)	0.0557(13)	-0.0037(3)	0.0567	-0.0047
2295.79317(4)	13	9	A2	12	9	A1	QR(12,9,A1)	0.0489(6)	-0.0019(3)	0.056	-0.0049
2302.16259(1)	14	9	A2	13	9	A1	QR(13,9,A1)	0.0453(10)	-0.0038(3)	0.055	-0.0051
2308.42967(1)	15	9	A1	14	9	A2	QR(14,9,A2)	0.0435(8)	-0.0042(4)	0.0537	-0.0052
2314.56879(3)	16	9	A1	15	9	A2	QR(15,9,A2)	0.0449(11)	-0.0026(3)	0.0522	-0.0053
2283.03699(3)	11	10	E	10	10	E	QR(10,10,E)	0.0550(13)		0.0544	-0.004
2289.67453(7)	12	10	E	11	10	E	QR(11,10,E)	0.0518(14)	-0.0005(4)	0.0552	-0.0044
2296.20201(3)	13	10	E	12	10	E	QR(12,10,E)	0.0502(12)	-0.0033(3)	0.0549	-0.0047
2302.61562(2)	14	10	E	13	10	E	QR(13,10,E)	0.0481(6)	-0.0052(3)	0.0543	-0.005
2308.90883(5)	15	10	E	14	10	E	QR(14,10,E)	0.0413(14)		0.0533	-0.0051
2290.38482(5)	12	11	E	11	11	E	QR(11,11,E)	0.0470(14)		0.0531	-0.0039
2296.91137(4)	13	11	E	12	11	E	QR(12,11,E)	0.0533(14)	-0.0006(3)	0.0536	-0.0045
2303.32369(1)	14	11	E	13	11	E	QR(13,11,E)	0.0440(10)	-0.0019(3)	0.0532	-0.0048
2297.69403(1)	13	12	A2	12	12	A1	QR(12,12,A1)	0.0477(6)		0.0518	-0.0039
2310.40514(4)	15	12	A1	14	12	A2	QR(14,12,A2)	0.0447(10)	-0.0037(3)	0.0515	-0.0049

[a]The values in parentheses represent two standard deviation uncertainties in the measured quantities in units of the last quoted digit.
[b]cm^{-1}.
[c]cm^{-1} atm^{-1} at 296 K.
[d]cm^{-1} atm^{-1} at the temperature of the spectra.
[e]The theoretical values are calculated using calculated broadening and shift coefficients reported in Refs. 9 and 10 and expression (3).

Table 3

All ^{Q}P and ^{Q}R transitions, and ^{Q}Q transitions with J" ≠ K		^{Q}Q transitions with J" = K	^{Q}Q transitions with J" = K+1
Band	ν_2	ν_2	ν_2
c_0	0.0649(4)	0.0687(6)	0.0671(9)
c_1	$-4.47(21)\times10^{-5}$	$-4.76(23)\times10^{-4}$	$-1.60(28)\times10^{-4}$
c_2	$-7.85(45)\times10^{-5}$	$1.49(17)\times10^{-7}$	$1.63(55)\times10^{-7}$
RMS error	3.5	1.1	1.5
#lines	303	11	12

The values in parentheses represent one standard deviation uncertainties in the measured quantities in units of the last quoted digit.